

AFGL-TR-82-0392

ATMOSPHERIC TRANSMITTANCE/RADIANCE
COMPUTER CODE FASCOD2

W.L. RIDGWAY
R.A. MOOSE
A.C. COGLEY

SONICRAFT, INC.
8859 S. GREENWOOD AVENUE
CHICAGO, ILLINOIS 60619

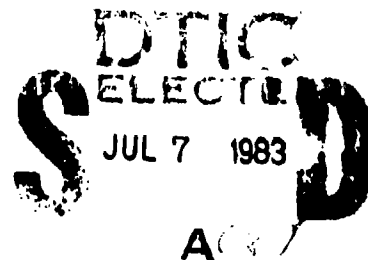
OCTOBER 1982

Final Report
(June 1979 - Oct. 1982)

Approved for public release; distribution unlimited

Prepared for:

AIR FORCE GEOPHYSICS LABORATORY
AIR FORCE SYSTEMS COMMAND
UNITED STATES AIR FORCE
HANSCOM AFB, MASSACHUSETTS 01731



83 07 044

ADA 130241
DTIC FILE COPY

Unclassified

SECURITY CLASSIFICATION OF THIS PAGE (When Data Entered)

| REPORT DOCUMENTATION PAGE | | READ INSTRUCTIONS BEFORE COMPLETING FORM |
|---|-----------------------|--|
| 1. REPORT NUMBER AFGL-TR-82-0392 | 2. GOVT ACCESSION NO. | 3. RECIPIENT'S CATALOG NUMBER |
| 4. TITLE (and Subtitle) ATMOSPHERIC TRANSMITTANCE/RADIANCE COMPUTER CODE FASCOD2 | | 5. TYPE OF REPORT & PERIOD COVERED Final Report (June 1979 to Oct. 1982) |
| | | 6. PERFORMING ORG. REPORT NUMBER |
| 7. AUTHOR(s) W. L. Ridgway R. A. Moose A. C. Cogley | | 8. CONTRACT OR GRANT NUMBER(s) F19628-79-C-0120 |
| 9. PERFORMING ORGANIZATION NAME AND ADDRESS Sonicraft, Inc. 8859 S. Greenwood Avenue Chicago, Illinois 60619 | | 10. PROGRAM ELEMENT, PROJECT, TASK AREA & WORK UNIT NUMBERS 62101F 767009AM |
| 11. CONTROLLING OFFICE NAME AND ADDRESS Air Force Geophysics Laboratory Hanscom AFB, Massachusetts Monitor/Francis X. Kneizys/OPI | | 12. REPORT DATE October 1982 |
| 14. MONITORING AGENCY NAME & ADDRESS (if different from Controlling Office) | | 13. NUMBER OF PAGES 94 |
| | | 15. SECURITY CLASS. (of this report) Unclassified |
| 16. DISTRIBUTION STATEMENT (of this Report) Approved for public release; distribution unlimited | | |
| 17. DISTRIBUTION STATEMENT (of the abstract entered in Block 20, if different from Report) | | |
| 18. SUPPLEMENTARY NOTES | | |
| 19. KEY WORDS (Continue on reverse side if necessary and identify by block number) Radiative Transfer High Spectral Resolution Thermal Radiation Atmospheric Radiance Non-LTE Radiative Transfer Continuum Absorption | | |
| 20. ABSTRACT (Continue on reverse side if necessary and identify by block number) This report continues the development of a line-by-line radiative transfer code for inhomogeneous, spherical atmospheres with refractive bending. Optical path calculations and properties for standard atmospheres are combined with the radiative transfer processes to form an integrated program. The code is then modified to include non-LTE effects on radiance and transmittance at the higher altitudes. For accurate continuum absorption near band heads, a new sub-Lorentzian form factor is developed that is compatible with the codes algorithm for line modeling. The CO ₂ continuum is | | |

DD FORM 1 JAN 73 1473

EDITION OF 1 NOV 65 IS OBSOLETE

Unclassified

SECURITY CLASSIFICATION OF THIS PAGE (When Data Entered)

Unclassified

SECURITY CLASSIFICATION OF THIS PAGE(When Data Entered)

studied as a particular example. All new computer coding and theoretical developments are documented and supported with example calculations.

1. TITLE
2. AUTHOR
3. PERIODICITY
4. DATE
5. PAGE
6. TOTAL
7. ABSTRACT
8. SUMMARY
9. REFERENCES
10. INDEXING
11. NOTES
12. COMMENTS
13. OTHER



Unclassified

SECURITY CLASSIFICATION OF THIS PAGE(When Data Entered)

TABLE OF CONTENTS

| <u>SECTION</u> | <u>PAGE</u> |
|--|-------------|
| 1. Introduction | 1 |
| 2. FASCOD2-80 Geometry and Aerosol Models | 4 |
| 2.1 Merging ATMPH with FASCOD1A | 4 |
| 2.2 Adding the LOWTRAN Aerosol Models to FASCOD1A | 8 |
| 3. Non-LTE Radiance and Transmittance: FASCOD2-82 | 16 |
| 3.1 Theoretical Development | 16 |
| 3.2 Non-LTE Code Modifications | 24 |
| 4. CO ₂ Continuum Absorption and Lineshape Models | 30 |
| 5. Layering in FASCOD | 46 |
| 5.1 Curtis-Godson Approximation | 46 |
| 5.2 Present Layering Procedure | 49 |
| 5.3 Recommendation for Further Studies | 52 |
| 6. Concluding Remarks | 53 |
| References | 54 |
| Appendix | |
| A. FASCOD2-80 User's Guide | 56 |
| A.1 Input Card Sequence and Format | 56 |
| A.2 Sample Run of FASCOD2-80 | 60 |
| B. FASCOD2-82 Program Revisions and User's Guide | 77 |
| C. Program BCDNLTE | 84 |
| C.1 Sample File for the Submission of BCDNLTE | 86 |
| C.2 Program BCNLTE: Listing of Subroutine VIBQU | 87 |

TABLE OF CONTENTS (cont'd)

LIST OF FIGURES

| | <u>PAGE</u> |
|---|-------------|
| FIGURE 2.1 Flow Diagram of Subroutine ATMPH | 7 |
| 2.2 Flow Diagram of Subroutine AERSOL | 12 |
| 3.1 Radiance in Units of Equivalent Blackbody Temperature for a 500 km path at 100 km Altitude Assuming LTE and Non-LTE Vibrational Populations | 25 |
| 4.1 Comparison of Sample FASCODE CO ₂ Transmittances | 43 |
| 4.2 Stratospheric Transmittance Spectrum From Balloon Observations, as compared to .. FASCOD2 | 44 |
| 4.3 Measured Atmospheric Transmittance over a 6.4 km path ... as Compared to... FASCOD2... .. | 45 |
| TABLE 4.1 FASCOD2 Lorentz Lineshape Subfunctions | 34 |
| 4.2 Comparison of Various CO ₂ Lineshape Form Factors | 40 |

1. INTRODUCTION

The Air Force Geophysics Laboratory, Optical Physics Division (AFGL,OPI) has been developing a high resolution radiative transfer code for direct point-to-point transmittance and radiance in the earth's atmosphere. This line-by-line spectral code uses the AFGL line atlas¹⁻³ and an algorithm called HIRACC⁴ to construct accurate radiative absorption properties. To permit computationally fast manipulation of the Voigt lineshape, an atmospheric transmittance and radiance model was developed called FASCODE⁵. A version of the resulting code along with certain external geometry and model atmosphere components was released for public use and called FASCOD1B⁶. This report develops and documents (incorporating work presented in Annual Reports 1 and 2^{7,8}) modules and subroutines for the generic code called FASCOD which will eventually be merged by AFGL into a integrated code to be designated FASCOD2.

The AFGL low resolution (typical resolution of about 20 wavenumbers) radiative transfer code, LOWTRAN 5⁹, contains extensive and well documented gaseous and aerosol model atmospheres. For consistency and certain possible intercomparisons, these same model atmospheres are built into FASCOD and this process is discussed in Section 2. The spherical geometry with refractive bending at the layer boundaries that has been used in the past by AFGL in LOWTRAN 5⁹, has now been modified¹⁰ by AFGL to include continuous refractive bending and a more accurate optical path routine. As part of Section 2 this new geometry package along with zeroth-order aerosol scattering and absorption are included in FASCOD. The modifications presented in Section 2 used an AFGL version of FASCOD called FASCOD1A,

and the resulting intermediate code is called FASCOD2-80 in this report.

For altitudes above 40 to 60 Km, certain molecular species can be found to have nonequilibrium population distributions in their vibrational states due to photo-driven chemistry and a reduced collision rate. Consequently the usual assumption of local thermodynamic equilibrium (LTE) that leads to the Planck function and absorption coefficient used for thermal radiation sources is not valid. Degges and Smith¹¹ have modeled such phenomena for selected vibrational transitions and have predicted non-LTE population densities for certain atmospheric conditions like daylight or night by season and location in the atmosphere (sun angle). Section 3 develops the necessary theory to calculate non-LTE transmittance and radiance and modifies FASCOD to execute in this mode when non-LTE population densities are supplied. Code changes are outlined and sample computational results presented.

Near band heads where the far wings of many superposed lines form an absorption continuum, the Lorentzian line shape does not predict correct results. This problem of the sub-Lorentzian line shape is discussed in Section 4 in the context of past work on theoretical modeling and experimental data. A new sub-Lorentzian form factor is developed that is compatible with the algorithm for line modeling in FASCOD and produces continuum absorption predictions for CO₂ that are as accurate as those using more complex form factors. The resulting code is documented and intermediate and final results using the developed form factor are presented and compared with other work in the literature. Because of continuous code developments at AFGL, the non-LTE and CO₂ continuum modifications were incorporated into FASCOD1B* (see Appendix B), and the resulting code is designated in this report FASCOD2-82.

*The CO₂ lineshape modifications developed in this report are presently available to the public in FASCOD1C.

Section 5 presents a discussion of the layering procedure used in FASCOD and how it may be improved. Such suggestions are not incorporated into the code. Finally, Section 6 contains a few summary remarks on how the various modules and subroutines developed here will be merged into an integrated code called FASCOD2.

2. FASCOD2-80 GEOMETRY AND AEROSOL MODELS

Here the radiative properties represented by the line modeling in FASCODE^{5, 6} are merged with gaseous and aerosol atmospheric models⁹ and the new spherical geometry package¹⁰ to produce a user oriented and automated code that calculates the atmospheric transmittance and radiance. The user's guide to the code and the results from example calculations are presented in Appendix A.

2.1 Merging ATMPATH With FASCOD1A: A new geometry routine called ATMPATH¹⁰ was developed at AFGL as an off-line program that prepared an atmospheric data file for FASCODE. The output of ATMPATH contains integrated absorber amounts and density weighted average temperatures and pressures for the homogeneous layers traversed by the optical path. Prior to the development of ATMPATH, programs called LAYER¹⁰ and DRIVER¹⁰ were run sequentially to prepare the same data. ATMPATH is more flexible and user oriented than its predecessors. A choice of seven (including one that may be supplied by the user) atmospheric models are provided, and the user specifies the placement of the layer boundaries. To automate execution, ATMPATH is made an on-line subroutine of FASCODE, and a discussion of this process follows.

Operation of ATMPATH and its subroutines is controlled by three input cards whose format is described in Appendix A. The first input card specifies the choice of model atmosphere. There are six built-in atmospheres specified by pressure, temperature and the molecular densities of H_2O , CO_2 , O_3 , N_2O , CO , CH_4 , O_2 and N_2 at 34 altitudes. These model atmospheres are essentially the same as those in LOWTRAN⁹, except that the densities are given in different units. One of the six model atmospheres stored in subroutine MDLATM, or a non-standard user-supplied atmosphere as

read by subroutine NSMDL, is selected and stored in the common block /MDATA/.

The second control card must contain three of the following five path parameters: H1, H2, ANGLE, RANGE, and BETA. The reader should refer to the LOWTRAN report⁹ for allowable combinations of these parameters. Next, the desired FASCODE layer boundaries are read in. These need not correspond to the altitudes contained in the model atmospheres or those of H1 and H2, the altitudes of the path end-points. The only restriction on the boundaries is that they be chosen such that the ratio of the mean half-widths in adjacent layers is not greater than 2 to 1.⁵ A new atmospheric profile containing both the previous altitudes and the desired FASCODE boundaries is formed. Pressures, temperatures, and molecular densities at these boundaries are found by interpolation of the model atmosphere.

Subroutine GMTRY is called next to calculate the refracted path through the atmosphere and to integrate the amounts of the absorbers along that path. Subroutine RFRPTH drives the integration and requires as input the set H1, ANGLE, H2 and LEN. These are determined by GMTRY using the three paths parameters supplied. A final atmospheric profile, generated by RFRPTH, starts at HMIN (tangent height if any) and goes up to MAX (H1, H2) (the larger of H1 and H2). The final profile is specified at H1, H2 and all of the model atmosphere altitudes and FASCODE layer boundaries between HMIN and MAX (H1, H2). The determination of the refracted path, integration of the absorber amounts, and formation of the homogeneous layers is done using all of the altitudes in the final profile as layer boundaries. Once the path and integrated amounts are known, layers are merged in ATMPH to form the desired FASCODE layers which are the boundaries HMIN, H1, H2 and

the FASCODE boundaries between HMIN and MAX (H1, H2). Note that the calculations of the refracted path and absorber amounts are done using the model atmosphere altitudes as additional layer boundaries. Only after the calculation procedure is complete, is the number of layers reduced. This is done to avoid degrading the model atmosphere data in the process of performing the path integrals. A general flow diagram on ATMPH is shown in Figure 2.1.

The addition of ATMPH as a subroutine of FASCODE was straightforward. A single statement in the FASCODE main routine was added to call ATMPH one time. During the execution of this call statement, all of the required atmospheric data is generated and stored in the common blocks /PATH/ and /OUTPUT/, which also appear in FASCODE subroutine PATH. PATH is called as before, first to initialize the binary line absorption file and then once for each layer to define the pressure, temperature, absorber amounts, and half-widths for that layer. Two changes in PATH are worth noting at this point. First, a new section of code was added to create and save the mean half-widths for all of the layers. This portion of code is executed during the first call of PATH when the line file is initialized. Second, layer data are now defined in terms of the stored array values. Statements of the following form have been added to the section of PATH that is executed for each layer

$$\text{PAVE} = \text{PBAR} (L) \quad (\text{average pressure}) \quad (2.1)$$

$$\text{TAVE} = \text{TBAR} (L) \quad (\text{average temperature}) \quad (2.2)$$

etc. ,

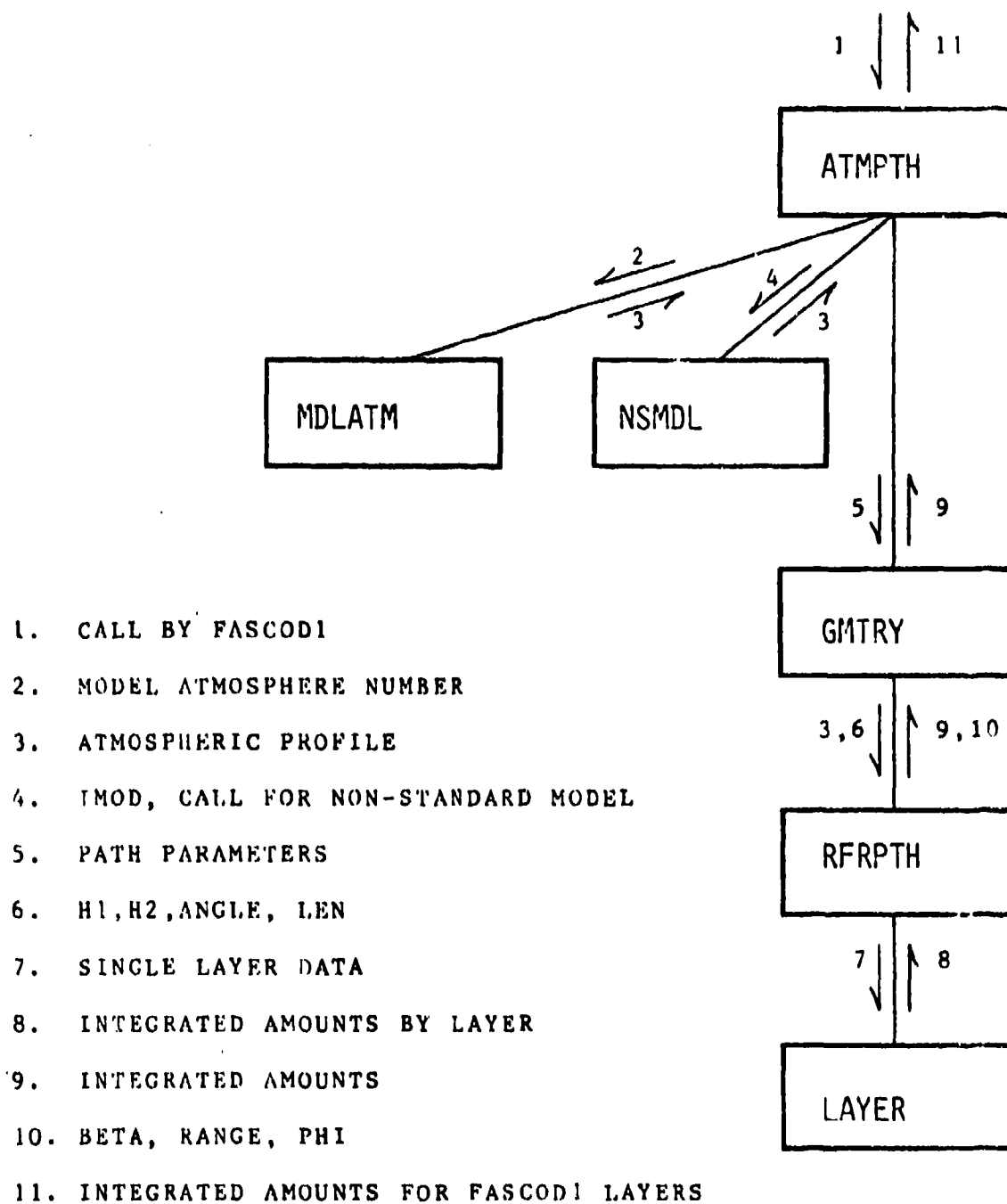


FIGURE 2.1 FLOW DIAGRAM OF SUBROUTINE ATMPTH

where L is the layer index. These quantities were previously read from a file generated by an off-line run of ATMPATH. The ATMPATH subroutine has no further interaction with FASCODE beyond the assignment of the average layer quantities in PATH.

To verify that ATMPATH had been successfully interfaced with FASCODE as a subroutine, comparison runs for horizontal, vertical, and slant (long and short) paths were made using the latest version of FASCOD2-80 with ATMPATH as a subroutine and an original version of FASCOD1 using ATMPATH as an off-line program. The codes produced identical output in all cases, indicating that the atmospheric information was being correctly transferred to FASCOD2 from the ATMPATH subroutine.

2.2 Adding the LOWTRAN Aerosol Models to FASCOD1A: In its original form, FASCOD1A did not include the effects of molecular scattering or aerosol scattering and absorption outside the microwave region. This extinction mechanism or zeroth-order scattering has been added as part of the development of FASCOD2-80. A single expression for the molecular scattering coefficient along with the complete set of AFGL aerosol models were taken directly from the LOWTRAN 5⁹ computer code. Linkage with FASCOD1 is accomplished with a newly written subroutine, AERSOL, which serves as a driver for LOWTRAN routines AERPRF, PRFDTA, EXABIN, EXTDTA, and AEREXT. The only changes made to these routines were to reduce the size and number of common blocks wherever LOWTRAN variables were not needed by FASCODE. AERSOL, its related subroutines, and the modifications made to FASCOD1A to incorporate the new extinction mechanism are documented here.

AERSOL is first called to generate the aerosol densities at the 34 standard altitudes of the model atmospheres. During this initial call a new

aerosol control card, described in Appendix A, is read. Subroutine AERPRF is then called 34 times (once for each altitude) to load the appropriate aerosol density profile from the data stored in subroutine PRFDTA into the array EHM(34) in common block /PROF/. These densities are unitless and are used to obtain equivalent sea level absorber amounts. At this point, control returns to FASCODE's main routine where ATMPATH is called to generate the layer data. EHM(34) is passed to ATMPATH where it is handled in the same manner as the molecular density profiles. The integrated aerosol amounts are stored in the array AWKAER(L) and are later assigned to the simple variable name WKAER in subroutine PATH. The primary function of the AERSOL routine, namely to generate the aerosol density profile and pass it to ATMPATH, is complete at this point.

AERSOL is subsequently called once for each layer. Its function now is to load the FASCODE arrays ABSRB and SCTTR with the additional required optical depths. ABSRB was previously used by FASCODE to store molecular continuum optical depths over the wavenumber range of VIABS to V2ABS in increments of DVABS. The aerosol extinction and molecular scattering optical depths were added to this array because they, like molecular continuum absorption, are relatively slow functions of wavenumber. The user should note that the array name "ABSRB" is now somewhat of a misnomer since scattering optical depths are also included. Renaming the array "EXTNCT" or "ABSSCT" to avoid any ambiguity is left to the user's discretion. The array SCTTR covering the same wavenumber region at the same resolution was empty prior to the current addition of the molecular and aerosol scattering optical depths. This array had been incorporated into an earlier version of the code with foresight of the current modifications.

Optical depths for the new mechanisms are defined as the product of the integrated amount and the appropriate attenuation coefficient. The aerosol amount for a given layer is WKAER. The coefficients are functions of the aerosol model, the relative humidity (for altitudes between 0 and 2 Km), and the wavenumber. During AERSOL's first call within the FASCODE layer loop, EXABIN is called to obtain a set of altitude and wavelength dependent attenuation coefficients using the data stored in subroutine EXTDTA. The resulting absorption and scattering coefficients are stored in arrays ABSC and EXTC. A wavenumber loop in AERSOL calls AEREXT repeatedly to determine the coefficients at the desired wavenumbers by interpolation of the ABSC and EXTC arrays. The aerosol extinction and scattering optical depths are then defined by expressions of the form:

$$\tau_{A, E} = EXT * WKAER \quad (2.3)$$

and

$$\tau_{A, S} = (EXT - ABS) * WKAER \quad (2.4)$$

If a FASCODE layer is not totally contained within one of the four aerosol altitude regions (0-2 Km, 2-10 Km, 10-30 Km, or 30-100 Km), a linear combination of coefficients is used. Molecular scattering is handled somewhat differently, although the basic idea is the same. Molecular amounts are measured in terms of equivalent sea level distances defined as

$$WKMOL = \left(\frac{P}{P_o} \right) \left(\frac{T_o}{T} \right) S, \quad (2.5)$$

where P and T are the molecular density weighted average pressure and temperature for the layer. The quantities P_0 and T_0 refer to STP, and S is the geometric path length through the layer. The scattering coefficient (per unit of sea level distance) is modelled by the following empirical expression.⁹

$$SCTM = v^4 / (9.26799 * 10^{18} - 1.07123 * 10^9 * v^2) \quad . \quad (2.6)$$

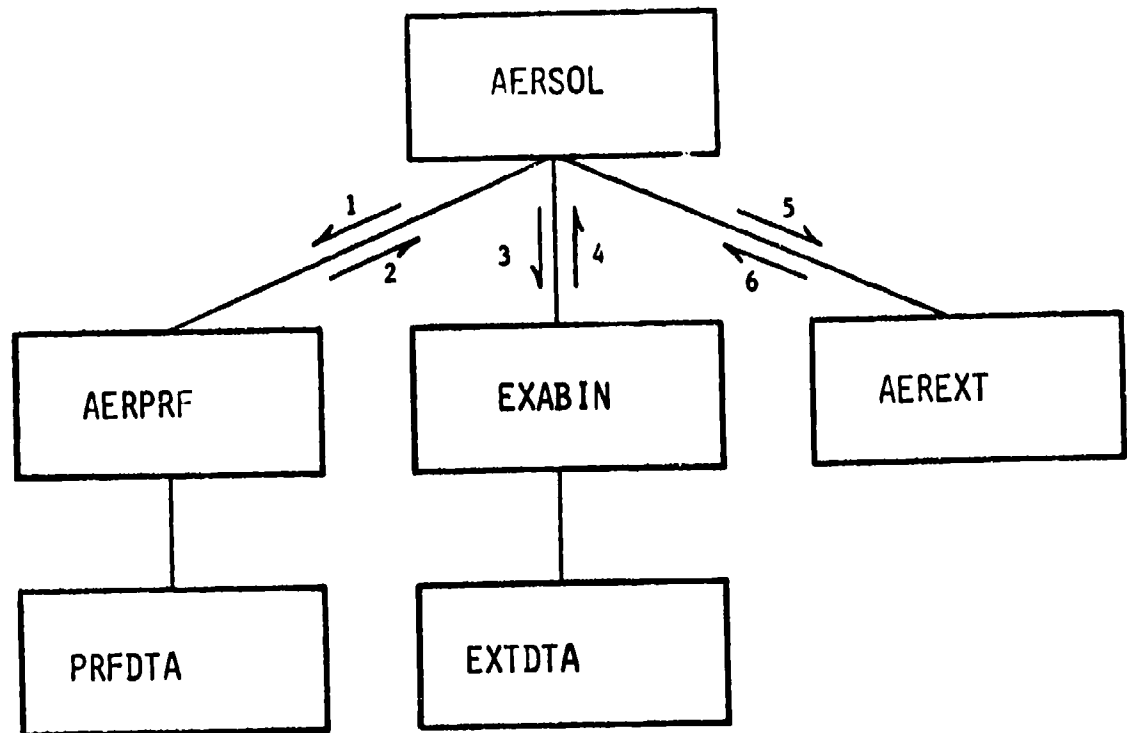
The molecular scattering optical depth is then given by the product of the coefficient and the "amount" as

$$\tau_{m, s} = SCTM * WKMOL \quad . \quad (2.7)$$

Loading the ABSRB and SCTTR arrays for each layer concludes the interaction of AERSOL with FASCODE'S main program. A flow diagram of AERSOL and its subroutines is shown in Figure 2.2.

As a result of adding the scattering mechanisms to FASCODE, the radiance algorithm required modification. The R1 array which contains the optical depths on the finest wavenumber grid ultimately has the ABSRB array merged into it. R1, therefore, now contains total extinction optical depths rather than just absorption. The transmission algorithm involves only exponentiation of the R1 array and remains unchanged. The radiance expression in subroutine EMIN was originally written as

$$BBRAD(I) = (1-TR(I)) * BB \quad (2.8)$$



1. CONTROL PARAMETERS
2. PROFILE EHM(34)
3. CONTROL PARAMETERS
4. ABSC(4,40), EXTC(4,40)
5. ABSC(4,40), EXTC(4,40)
6. ABSV(4), EXTV(4)

FIGURE 2.2 FLOW DIAGRAM OF SUBROUTINE AERSOL

and is now incorrect because TR(I) is an extinction rather than an absorption transmittance. The expression is easily corrected by multiplying it by the ratio of absorption to extinction. It turns out to be more convenient to use unity minus the ratio of scattering to extinction. This is expressed in the code as

$$\text{BBRAD(I)} = (1 - \text{TR(I)}) (1 - \text{ALB}) * \text{BB} , \quad (2.9)$$

where ALB is the ratio of scattering to extinction optical depths, i.e. the single scattering albedo. Notice that equation (2.9) reduces to equation (2.8) in the limit of zero scattering.

To verify that the aerosol routines were functioning correctly as part of the FASCODE program, comparisons were made with LOWTRAN⁹ results. FASCODE and LOWTRAN now contain identical aerosol models, but the molecular absorption processes are, of course, completely different. To obtain comparable data from FASCODE, the molecular absorption was artificially suppressed and additional output was written. Vertical paths were chosen to eliminate any differences caused as a result of the different geometry routines used in the two codes. Comparisons of aerosol absorber amounts, coefficients, and transmittances indicated excellent agreement between FASCODE and LOWTRAN. A slight difference in the aerosol coefficient in the 0-2 Km boundary layer region was observed and attributed to the different relative humidity calculations within the two codes. The relative humidity algorithm developed under this contract for use with FASCODE differs from the one currently used in LOWTRAN. Although the net effect on the aerosol coefficients is small, typically

about one percent, it does lead to differences in the attenuation coefficients when used as a reference point for interpolation of the stored data. The following brief description of the two algorithms will illustrate the fundamental differences and how they may be eliminated.

The LOWTRAN geometry routines integrate the relative humidity, weighted by the aerosol density, while performing the usual path integrations. The calculation is the numerical approximation of

$$\overline{RH} = \frac{\int_0^2 RH(h) * WK(h) dz}{\int_0^2 WK(h) dz} , \quad (2.10)$$

where RH and WK are arrays containing the relative humidity and aerosol density profiles as a function of altitude h, and dz is the incremental path length. Both the numerator and denominator of Eq. (2.10) are formed during the geometry calculations and then their quotient is formed. By contrast the FASCODE relative humidity calculation occurs after all geometry calculations are completed. A discrete sum of layer properties rather than "integration" of atmospheric profiles is used. The average relative humidity is expressed as

$$\overline{RH} = \frac{\sum_{0-2 \text{ Km}} RH(L) WK(L)}{\sum_{0-2 \text{ Km}} WK(L)} , \quad (2.11)$$

where RH and WK are arrays containing the relative humidity and aerosol absorber amounts for the FASCODE layers. Equations (2.10) and (2.11) both represent an aerosol weighted relative humidity. As it turns out, the denominators of the two expressions are numerically equivalent. The difference lies in the numerators, with the sum in Equation (2.11) being an approximation of the integral in Equation (2.10). Although time and resources did not permit the replacement of FASCODE'S relative humidity algorithm with the more accurate one found in LOWTRAN, a method to do so is outlined below for future reference:

1. Provide additional array space for the relative humidity profile and a weighted relative humidity sum.
2. Add a section of code prior to the geometry calculations to generate and load the relative humidity profile.
3. Modify the geometry routines to perform an additional integration, namely, the relative humidity weighted by the aerosol density. Note, this integration need only cover the 0-2 Km boundary layer region.
4. After the geometry calculations are completed, divide the weighted relative humidity sum by the boundary layer aerosol amount.

3. NON-LTE RADIANCE AND TRANSMITTANCE: FASCOD2-82

In this section we review the monochromatic radiative transfer properties of an absorbing gaseous medium which may not be in local thermodynamic equilibrium (LTE). Those assumptions and relationships which are valid only under LTE circumstances are distinguished from the quite general aspects of radiative transfer. The transfer equation describes the influence which the atmospheric environment (the optical medium) has on the radiation field through both losses and emission, the problem which FASCOD2 has been designed to address. The radiation field also affects, in various ways, the state of the gas, both as a driving force that stimulates molecular transitions and as a mechanism for energy exchange and relaxation within the medium. The largest single effect of solar radiation on the earth's atmosphere is simple thermal heating. However, in the upper atmosphere selectively enhanced molecular excitations and sun-driven photochemical processes combine with the slower relaxation rates of the rarefied gas medium to drive the medium away from a state of thermodynamic equilibrium.

3.1. Theoretical Development: High altitude radiance measurements have confirmed that certain species, notably water vapor, carbon dioxide, ozone, and nitric oxide, may be found in non-LTE states above an altitude of about 40 - 60 km (even lower for NO).¹¹ In the upper atmosphere, it is necessary to account for these non-equilibrium states of the optical medium if the radiative transfer is to be properly modeled. At lower altitudes, the LTE assumption is generally valid, although the local

temperature remains a strong function of altitude from the boundary mixing layer to the upper stratosphere.

FASCOD2 calculates only the unscattered radiative intensity for a particular direction of observation using known atmospheric properties. The code therefore implicitly decouples the problem of solving for these intensities from the problem of finding the state of the medium itself. For conditions of local thermodynamic equilibrium, the properties of an atmosphere which are needed to perform these calculations (using LTE relationships) are accessible in the form of stored atmospheric profiles (temperature, pressure, gas densities) plus an off-line file containing molecular line data at $T=296^{\circ}\text{K}^1$. The non-LTE problem however, requires a more detailed description of the propagating medium, and removal of all LTE assumptions used in the radiative transfer algorithm.

The non-LTE transfer problem can be described by the following quite general governing equation for the monochromatic radiative intensity I_{ν} :

$$\frac{dI_{\nu}}{ds} = K_{\nu} I_{\nu} + R_{\nu} . \quad [3.1]$$

The variable s is taken to be the length along a (possibly curved) line-of-sight through the atmosphere. (This could equally well have been defined as a molecular amount per unit cross-sectional area or gas column density.) The local monochromatic volumetric extinction coefficient is K_{ν} , and R_{ν} represents the source term for radiative emission per unit length. It is important to note that both K_{ν} and R_{ν} are linear func-

tions of the densities of each IR-active gas and aerosol constituent. Therefore, the separate contributions to both quantities can be added line-by-line, molecule-by-molecule, aerosol-by-aerosol, etc.

The basic objective is to calculate the contribution to both K_v and R_v for all molecular absorption/emission lines. In order to illustrate the processes involved, a representative vibrational-rotational transition is considered between an upper state u and lower state l corresponding to a spectral line centered at frequency ν_0 . In terms of the standard Einstein coefficients B_{lu} , B_{ul} , and A_{ul} , for absorption, stimulated, and spontaneous emission, respectively, the volumetric absorption and radiance for this transition are given by

$$K_v = \frac{h\nu}{4\pi} (B_{lu} n_l \phi_v - B_{ul} n_u \psi_v) \quad [3.2]$$

and

$$R_v = \frac{h\nu}{4\pi} A_{ul} n_u \chi_v. \quad [3.3]$$

The quantities ϕ_v , ψ_v , and χ_v represent distinct lineshape functions of the spectral distance $(\nu - \nu_0)$, and are referenced to one another by having $\phi(0) = \psi(0) = \chi(0)$. Number density populations of the lower and upper V-R states are given by n_l and n_u , respectively.

The Einstein coefficients are a set of rate constants which are specific to a particular transition, but which are not independent. This fact is generally true and most easily demonstrated by considering a situation

of complete equilibrium. At equilibrium the radiation field within a sufficiently large medium of temperature T is isotropic and has a spectral intensity given by the Planck function $B_\nu(T)$ in the form

$$B_\nu(T) = \frac{2h\nu^3}{c^2(e^{h\nu/kT} - 1)} \quad [3.4]$$

Additionally, the populations of the upper and lower states have the ratio

$$\frac{g_l n_u^e}{g_u n_l^e} = e^{-h\nu_0/kT} \quad [3.5]$$

given by the Boltzmann distribution for the temperature T . The constant integer g 's are single state degeneracy factors. The superscript "e" will be used throughout to denote the equilibrium state for a specified temperature. Since the intensity doesn't change with position in this case, the equation of transfer reduces to

$$R_\nu = K_\nu B_\nu(T) \quad , \quad [3.6]$$

which implies that at equilibrium

$$A_{ul} n_u^e \chi_\nu = [B_{lu} n_l^e \phi_\nu - B_{ul} n_u^e \psi_\nu] B_\nu(T) \quad [3.7]$$

Furthermore, the fundamental symmetry of the quantum matrix elements for the processes of absorption and stimulated emission requires that $g_u B_{ul} = g_l B_{lu}$. Considering Equations 3.4, 3.5, and 3.7 evaluated at the line center point $\nu = \nu_0$, the three Einstein coefficients can be expressed as

$$B_{lu} = g_u \bar{B}$$

$$B_{ul} = g_l \bar{B}$$

[3.8]

$$A_{ul} = \frac{2h\nu^3}{c^2} g_l \bar{B} ,$$

where \bar{B} is a single rate coefficient.

The above argument can also be used to relate the lineshapes to one another. There is a primary relationship between emission lineshapes $\chi_\nu = \psi_\nu$ which follows from the Wiener-Khintchine theorem and possibly more general arguments as well.^{13, 14} One also has from Equations 3.5, 3.7, and 3.8 that

$$\chi_\nu = \frac{e^{h\nu_0/kT} \phi_\nu - \psi_\nu}{e^{h\nu/kT} - 1} ,$$

[3.9]

or equivalently

$$\chi_\nu = \psi_\nu = \phi_\nu e^{-h(\nu - \nu_0)/kT}$$

[3.10]

therefore requiring only a single lineshape model to be used in describing the three radiative processes. Arguments similar to the one above have been made previously. Gilles¹⁵ develops the corresponding lineshape relationships using a different lineshape normalization condition and somewhat different notation throughout.

In summary, the equilibrium single-line radiative problem within a given medium can be adequately described in terms of a single rate coefficient (or linestrength) and a single lineshape assumed known from other considerations. The above Einstein coefficients can be applied to the non-LTE problem with equal validity since they represent molecular properties. Any one of several assumptions can be made regarding how the lineshapes should be related to each other under non-LTE conditions, that is, how (3.10) can be generalized. In view of the fact that both collisional and Doppler line broadening mechanisms depend largely on the bulk thermodynamic properties of pressure and temperature, and not on other degrees of freedom such as the particular V-R state populations n_l and n_u , it seems reasonable to assume that the lineshapes should have their LTE form even under non-LTE conditions. One then only requires detailed knowledge of all V-R single state populations to solve the radiative transfer problem by applying Equations 3.2, 3.3, 3.8, and 3.10.

In carrying out calculations based on the above theory, it becomes rather awkward to actually allow ϕ_ν and ψ_ν to be different lineshape functions. The overall (true absorption minus induced emission) lineshape for absorption is a weighted difference between the functions ϕ_ν and ψ_ν , and would therefore change as the upper to lower state population ratio changes with altitude and from line to line. To avoid this complication, the approximation is made that the overall (net) absorption lineshape is the same under non-LTE conditions as it is under LTE conditions. From (3.10) it can be seen that this approximation introduces errors in the lineshape wings of order $\exp[-h(\nu - \nu_0)/kT]$. Except for the microwave region, the errors introduced by this lineshape approximation

are quite small in comparison to the typical uncertainties in the non-LTE linestrengths. The differences are especially insignificant for the narrow Doppler lines found at high altitudes.

With the above approximation, the single-line volumetric absorption and local thermal radiance is given by

$$K_v = \frac{h\nu}{4} \bar{B} (g_u n_l - g_l n_u) \phi_v \quad [3.11]$$

and

$$R_v = \frac{h^2 \nu^4}{2\pi c^2} \bar{B} g_l n_u \chi_v \quad [3.12]$$

This result is a general one for a two-level system. The lineshapes are functions of the bulk thermodynamic quantities such as pressure, temperature, plus individual gas densities which can separately influence the far wing lineshapes. The populations are given by the Boltzman distribution only under conditions of local thermodynamic equilibrium. In the presense of a strong radiation field, or under conditions where relaxation rates are small, the upper and lower state populations will often bear no simple relationship to each other. Therefore, the absorption and radiance owing to any single transition (and to all transitions of all molecules) are no longer simply related for a non-LTE atmosphere, and more specifically, the radiance from such an optically thick atmosphere will not be given by the Planck function.

In the upper atmosphere, relaxation rates for the different excitation modes of various molecules are found to vary considerably. Rotational

degrees of freedom generally relax much more rapidly to a state of thermal equilibrium than do vibrational modes. The work of Degges and Smith¹¹ makes use of this fact in order to construct a high altitude model which calculates vibrational state populations, while assuming that the rotational state populations are thermally distributed within each vibrational state according to the Boltzman distribution for the translational (bulk) temperature. This model employs a single kinetic temperature which is a function of altitude, plus a set of vibrational state population variables which are found by solving a model for the coupled gas-radiation field problem.

These vibrational population variables can be used to relate the non-LTE single-line absorption and radiance to the same quantities calculated for an atmosphere in equilibrium at the kinetic temperature. The relationship between equilibrium and non-equilibrium radiative properties for a single line can be summarized by

$$\text{and } K_v = \left[\frac{g_u n_l - g_l n_u}{g_u n_l^e - g_l n_u^e} \right] K_v^e \quad [3.13]$$

$$R_v = \frac{n_u}{n_e} R_v^e, \quad [3.14]$$

which can also be written in terms of the Planck function as

$$R_v = \frac{n_u}{n_e} B_v(T) K_v^e. \quad [3.15]$$

In the upper atmosphere under non-LTE conditions, some vibrational state populations are increased by as much as a factor of 100 to 1000 over LTE populations. The ground (lowest energy) vibrational state is usually only marginally depleted. The net effect, as can be seen from 3.13 and 3.15, tends to be a slightly diminished spectral absorption coefficient, while the radiance tends to be markedly, though selectively, enhanced in some bands of ozone, carbon dioxide, nitric oxide, and water vapor. The other major gases are also affected to a lesser extent.

Some sample calculations have been made using this high resolution non-LTE model. Figure 3.1 shows the enhancement of the predicted radiance by non-equilibrium vibrational populations which would be seen by an observer looking along a 500 km horizontal path at an altitude of 100 km, based on the 1962 U.S. Standard Atmosphere in the model of Degges and Smith. The comparison of LTE and non-LTE calculations is made for a spectral region within the 4.3 micron band of CO_2 . This band and others often show radiance enhancements by several orders of magnitude over what could be expected of a gas at thermal equilibrium.

3.2. Non-LTE Code Modifications: The relations derived in the previous section provide for the calculation of absorption and radiance spectral functions using two separate line-by-line convolutions. (The two sums would be related by the Planck function in the equilibrium limit.) The non-LTE algorithm of FASCOD2 calculates K_ν directly, but the radiance is computed from a line-by-line sum of the quantity C_ν defined by

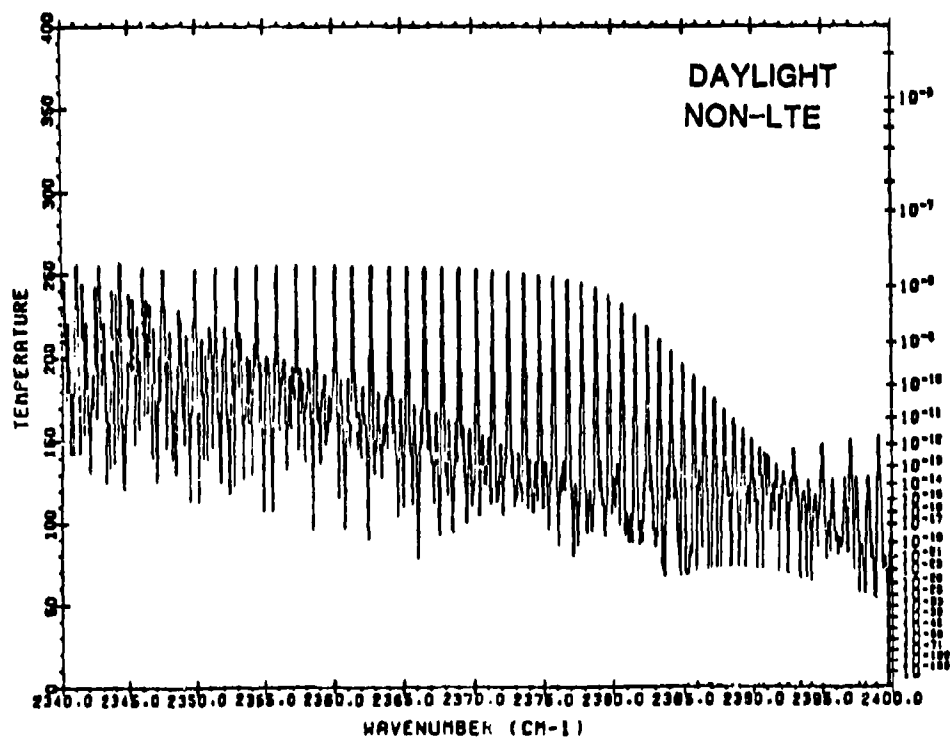
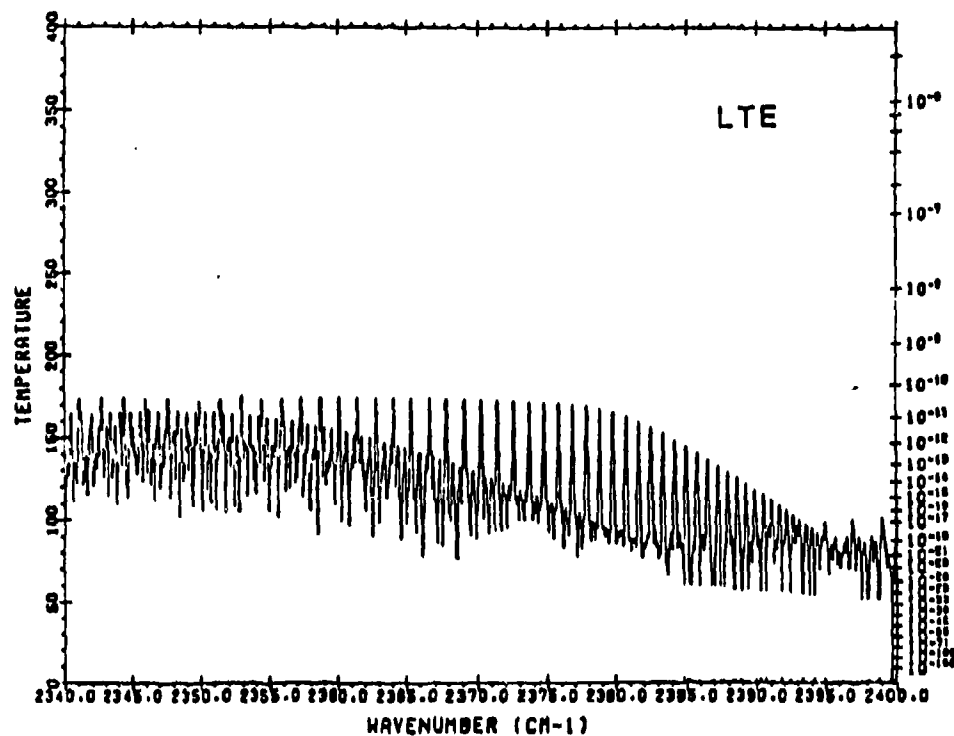


Figure 3.1 Radiance in Units of Equivilent Blackbody Temperature for a 500 km Path at 100 km Altitude Assuming LTE and Non-LTE Vibrational Populations

$$C_v = K_v - \frac{R_v}{B_v(T)} \quad , \quad [3.16]$$

which can be viewed as representing that part of the non-LTE absorption which is not returned to the radiation field as thermal emission. Any two of the spectral functions K_v , R_v , and C_v can easily be used to obtain the third, so the choice of summing C_v rather than R_v has been made for computational reasons. C_v can be seen to vanish in the equilibrium limit, and furthermore, in an atmosphere of mixed gases, only transitions of those gases which are not in thermal equilibrium will contribute to C_v . This property is used by FASCOD2 to shorten the second line-by-line sum where possible.

To compute the absorption and radiance for optical path segments in the upper atmosphere, FASCOD2 employs the vibrational population model of Degges and Smith¹¹. Each IR line corresponds to a transition between two molecular vibrational states. The identification of these two states is made by program BCDNLTE, a separate routine modeled after BCDMRG⁵, which prepares a blocked line data file for FASCOD2. The population of each vibrational state is referenced to its equilibrium value, calculated at the kinetic temperature T . The ratios of non-LTE vibrational populations to their reference values are given by the enhancement (or depletion) ratios

$$r_l = \frac{n_l}{n_l^c} \quad \text{and} \quad r_u = \frac{n_u}{n_u^e} \quad , \quad [3.17]$$

The fact that rotational sub-states are thermally distributed has been used to relate the vibrational state population ratios directly to single V-R state population ratios. That is, rotational partition functions and Boltzman factors produce a factor of unity in the V-R ratios. The single-line contributions to K_v and C_v can be expressed simply in terms of these ratios according to

$$K_v = \left[\frac{r_\ell - r_u \Delta}{1 - \Delta} \right] K_v e \quad [3.18]$$

and

$$C_v = \left[\frac{r_\ell - r_u}{1 - \Delta} \right] K_v e \quad , \quad [3.19]$$

where Δ is the Boltzman factor,

$$\Delta = \frac{g_\ell n_u e^{-h\nu_o/kT}}{g_u n_\ell e} = e \quad [3.20]$$

The two factors in brackets can be viewed as non-LTE linestrength correction factors for these absorption and "effective absorption" line-by-line calculations.

To summarize, if "i" denotes a single absorption line of a particular molecular species, the two functions K_v and C_v are obtained by performing the two sums

$$K_v = \sum_i K_v^i \quad \text{and} \quad C_v = \sum_i C_v^i \quad [3.21]$$

which are taken over all lines of all molecules in the case of K_v , and over all lines connecting non-equilibrium vibrational populations in the case of C_v . Both K_v and C_v employ the same approximate equilibrium lineshape functions as discussed above. The complete solution of the radiative transfer equation for a path of length L through each homogeneous layer, including self-absorption of emitted radiation, is given by

$$I_v = I_v^0 e^{-K_v L} + B_v \left[1 - \frac{C_v}{K_v} \right] \left[1 - e^{-K_v L} \right]. \quad [3.22]$$

The effect of solving the non-equilibrium problem in each homogeneous layer has been to modify the linestrengths contributing to the local absorption coefficient K_v , and to replace the Planck function B_v by the high resolution function $B_v [1 - C_v / K_v]$.

In the remainder of this section, the new procedures that are necessary to make FASCOD2 perform the non-LTE calculations are outlined. Most of the modifications when considered individually have been relatively minor, with the exceptions that one new subroutine was introduced (RDPOPS) and an entire new branch of the program (HIRACQ and subroutines) was created to mimic HIRAC in performing two line-by-line calculations rather than one. These modifications are described in detail in Appendix B. A list of the new procedures follows:

- (1) Identify and label those upper and lower state vibrational states of each spectral line which are non-thermally populated [BCDNLTE].

(2) Read the non-LTE vibrational state population data given by the model of Degges and Smith, and compute the population enhancement ratio for each vibrational state [RDPOPS].

(3) In computing K_v , modify the single-line absorption linestrength according to Equation 3.18 [HIRACQ].

(4) Perform a second line-by-line calculation of the "effective absorption" function C_v patterned after the actual absorption, but based on (3.19), including only those lines identified in (1) as having either upper or lower state non-equilibrium populations [HIRACQ].

(5) Modify the radiance calculation in each layer to use the non-LTE form of the Planck function $B_v [1 - C_v / K_v]$ [EMIN].

4. CO₂ CONTINUUM ABSORPTION AND LINESHAPE MODELS

The line-by-line HIRACC molecular absorption algorithm⁴ has been extended to include the lineshape region within 256 halfwidths of the line center of each spectral line.^{5, 6} The primary consideration in extending the lineshape bound outward from 64 halfwidths was to better fit the band edge and region of continuum absorption thought to arise primarily from the cumulative contribution from the far wings of many overlapping lines. The continuum absorption is known to scale nearly linearly with both the gas amount and the broadening gas density (more precisely, the molecular collision frequency) in the high pressure (Lorentz shape) limit^{15, 16} It can therefore be modelled by scaling a precomputed or measured continuum function based on a reference pressure and temperature. The process can be complicated if multiple broadening mechanisms must be accounted for, as in the case of self and foreign gas broadening of water vapor lines. The water vapor continuum has been the focus of considerable work at AFGL and is discussed in Reference [6].

In order to model the CO₂ continuum at typical atmospheric mixing ratios, it has been assumed that CO₂ self broadening can be neglected in favor of the much stronger foreign gas (principally nitrogen) broadening effects. A number of measurements have established that the collisional broadening mechanism (whether self or foreign) gives rise to a CO₂ line shape which falls off much more rapidly in the far wings than can be accounted for by the Lorentz lineshape function.^{15, 16} This sub-Lorentzian

behavior is particularly evident just above the band head of the CO₂ 4.3 micron band. Estimates of the spectral absorption in this region, if based on a Lorentz lineshape, can be in error by as much as a factor of 3. More recent atmospheric transmittance measurements made at sea level¹⁷ and also from high altitude balloons¹⁸ confirm the sub-Lorentzian behavior of line wings above the 4.3 micron band edge from about 2380 to 2420 CM-1.

Several explanations for the sub-Lorentzian shape in the line wings have been suggested. They range from arguments for a modified impact approximation¹⁹ which is needed to account for the finite interaction times of molecular collisions, to the suggestion that CO₂-N₂ dimer effects play an important role.²⁰ Other theoretical models have been suggested but will not be summarized here. See, for example, [22] and [23]. These models provide an important framework within which the measurements obtained to date can be considered, but compelling evidence for any single model has been lacking and each model has had limited usefulness as a predictive tool.

The most useful sub-Lorentzian lineshape models to date have been empirical. The usual approach has been to modify the Lorentzian lineshape function with a multiparameter form factor which is obtained by fitting experimental data with trial synthetic absorption spectra. Winters, Silverman, and Benedict (hereafter shortened to WSB) first used an exponential form factor for nitrogen broadening given by

$$\exp \left[- 0.46 (|\nu - \nu_0| - 5.0)^{0.46} \right] , \quad [4.1]$$

which falls off smoothly starting at 5 wavenumbers from the line center and has two adjustable parameters.¹⁵ Susskind and Mo have also used this functional form, but they adjusted it to fall off at only 0.5 wavenumbers from line center, and fitted the exponential WSB form with somewhat different parameters using the form factor

$$\exp \left[- 0.601 (|\nu - \nu_0| - 0.5)^{0.434} \right] \quad [4.2]$$

to accomplish the same task.²³ Burch et. al. suggested that a more complicated numerical form factor which also starts to fall off within one wavenumber of the line center was needed and they proceeded to construct separate form factors for both self and foreign gas broadening near the three CO₂ bands at 4.3, 2.6, and 1.4 microns.¹⁶ Recently, Cann et al have restudied the problem and suggested a different numerical form factor based on similar considerations.^{24, 25}

The available laboratory data are not clearly inconsistent with any of these models, yet there are seemingly significant differences among the four form factors mentioned above. In particular, the shape of the form factor for the spectral region within 10 wavenumbers of line center varies considerably among these models. Experience in building synthetic continuum absorption models such as these has shown that single-line features are usually blurred when the wing contributions from many lines are superposed. This fact suggests that it may not be possible to extract a unique form factor from the relatively few laboratory band-edge absorption measurements which are available.

Atmospheric transmittance measurements also shed some light on the distinctions among the model predictions. Smith et al have recently compared the continuum transmission predicted by these models to balloon measurements of stratospheric solar transmission¹⁸. Their comparison favors the two models of Burch et al and Susskind and Mo, but some uncertainty is introduced by the presense of the pressure induced nitrogen absorption continuum and by the fact that the strongest part of the CO₂ continuum above the 2397 CM-1 band head is compressed into a smaller spectral region at the lower stratospheric pressures where these data are taken. NRL atmospheric measurements taken over a 5.1 km path at sea level include the same nitrogen continuum, plus a somewhat uncertain water vapor continuum contribution in the same region and significant aerosol extinction along the optical path.^{17, 24, 25} However, in spite of the numerous overlapping contributions, Cann et al do claim an improved fit to the NRL data using their own CO₂ form factor.

In view of the variety of empirical lineshapes that have been used to fit the CO₂ continuum, it was decided that a new two-parameter exponential-type form factor particularly suited to the HIRACC algorithm would be studied for incorporation into FASCOD2. We will briefly review below the relevant features of the HIRACC line-by-line calculation before detailing the CO₂ form factor which has been used. The reader is referred to [5] and [6] for more complete descriptions of the HIRACC algorithm.

HIRACC approximates the Voigt lineshape by a weighted sum of Lorentz and Gaussian (Doppler) lineshapes. The relative weight of each component is determined by the Voigt parameter δ , defined in terms of the Lorentz

and Doppler halfwidths according to

$$\delta = \frac{\alpha_L}{\alpha_L + \alpha_D} \quad [4.3]$$

The Lorentz function is numerically constructed by the superposition of as many as four subfunctions. A summary of the functional forms for the different domains of each subfunction is given in Table 4.1. Note that the parameter X is the distance from line center measured in halfwidths.

The notable functional forms are:

| | |
|---------|--|
| L(X) | Lorentz function. |
| Q4(X) | The quartic function whose value, slope, and curvature match the Lorentzian at $X=4$. |
| Q16(X) | The quartic function fitting L(X) at $X=16$. |
| Q64(X) | The quartic function fitting L(X) at $X=64$. |
| Q256(X) | The quartic function fitting L(X) at $X=256$. |

TABLE 4.1 FASCOD2 LORENTZ LINESHAPE SUBFUNCTIONS

| DOMAIN | F1 | F2 | F3 | F4 | REMAINDER |
|----------------|------|--------|---------|--------------|-----------|
| $X < 4$ | L-Q4 | Q4-Q16 | Q16-Q64 | Q64-L(X=256) | L(X=256) |
| $4 < X < 16$ | 0 | L-Q16 | Q16-Q64 | Q64-L(X=256) | L(X=256) |
| $16 < X < 64$ | 0 | 0 | L-Q64 | Q64-L(X=256) | L(X=256) |
| $64 < X < 256$ | 0 | 0 | 0 | L-L(X=256) | L(X=256) |
| $256 < X$ | 0 | 0 | 0 | 0 | L |

The sum of the four subfunctions is the Lorentz function minus its value at $X=256$ for the domain within 256 halfwidths of the line center, while the sum is zero outside 256 halfwidths. The column labelled "REMAINDER" shows the "fifth" function which would be needed to complete the Lorentz shape in each domain.

The advantages of the multifunction construction have been discussed previously⁵. In particular, as the domain of each successive subfunction grows larger, the functions F_1 , F_2 , etc. grow successively smoother, so that the wavenumber grid on which each function is specified can contain approximately the same number of points. FASCOD2 uses these subfunctions to synthesize the single layer absorptive optical depth through line-by-line summations. Note that each subfunction has a different characteristic resolution, so that it is advantageous to carry out five separate line-by-line sums in order to construct five partial-absorption spectra (designated R_1 , R_2 , R_3 , R_4 , and ABS in the program) which are defined on successively coarser wavenumber grids. Once the five convolutions are completed, they are merged into a single optical depth function which has the high resolution characteristic of F_1 .

The manner in which the five sums are actually computed deserves some discussion. The sums R_1 , R_2 , and R_3 , which make up nearly all of the line contribution to band absorption, are computed line-by-line for each absorbing gas by HIRACC and its subroutines. The rather low resolution function R_4 is computed by subroutine LBLF4 and its subroutines. These four line-by-line convolutions use individual line strengths and halfwidths which are computed in each atmospheric layer from the average layer pressure and

temperature, and the line file data. The REMAINDER or "fifth" subfunction, however, has been used only to precompute the total contribution of all lines to the continuum at standard temperature and pressure. When the fifth partial-absorption function "ABS" is required in each layer, this stored continuum function is scaled according to

$$\text{ABS}(P,T,\text{GNU}) = \text{ABS}(P_0,T_0,\text{GNU}) \left[P/P_0 \right] \left[T_0/T \right]^{0.5}, \quad [4.4]$$

which approximately reflects the dependence of the far wing absorption on collision frequency.

The problem of finding an adequate model for the far wing CO_2 lineshape was first studied using the simple exponential form factor (following references [16] and [24]) with the lineshape

$$\begin{aligned} L(X) \exp\left[-A (\text{DELTA}-C)^B \right] & \quad \text{for} \quad \text{DELTA} > C \\ L(X) & \quad \text{DELTA} < C \end{aligned}$$

having adjustable parameters A, B, and variable "turn-on" point C. DELTA is the spectral distance from the line center measured in wavenumbers. Trial CO_2 absorption spectra built using the exponential-type lineshape were found to fit the data progressively better as C was decreased from the WSB value of 5 wavenumbers to 1 wavenumber, and finally to 0.5 wavenumbers. The fits suggest that a very small value of C works best. However, one knows that the continuum absorption is quite insensitive to the lineshape within a few halfwidths of the line center. One might conclude that the "turn-on point" should not be chosen simply from considerations based on fitting the continuum, since the small value of C may prove to be an arti-

fact of forcing the form factor to be of the exponential type rather than a meaningful result. Additionally, one risks altering the integrated line-strength if the "turn-on point" is too close to the line center. With the use of a value of $C \ll 1$, it could become necessary to renormalize the line strengths in order to handle this difficulty consistently.

A quite different CO_2 lineshape model has actually been implemented in FASCOD2. This was done partly to avoid the difficulty of fixing the "turn-on" point for sub-Lorentzian behavior, and partly out of considerations related to the computational complexities involved in modifying all of the sub-functions. The sub-Lorentzian form of the lineshape was accounted for by multiplying only two of the five Lorentz lineshape subfunctions, namely F4 and the REMAINDER or fifth subfunction, by the single exponential-type form factor CHI given by

$$\text{CHI}(\text{DELTA}) = \exp\left[-A (\text{DELTA})^B\right], \quad [4.5]$$

and A and B are adjustable parameters. Modification of only the last two subfunctions with this form factor produces a CO_2 lineshape given by

$$[F1 + F2 + F3] + \text{CHI}(\text{DELTA}) [F4 + \text{REMAINDER}].$$

From Table 4.1, it is clear that this model is equivalent to a lineshape specified by

$$L(X) = [1 - \text{CHI}(\text{DELTA})] Q64(X) \quad \text{for} \quad X < 64$$

and

$$\text{CHI}(\text{DELTA}) L(X) \quad \text{for} \quad X > 64.$$

This lineshape was used to construct a number of trial synthetic CO₂ absorption spectra over the region between 2380 and 2500 CM-1. The various continua were compared to laboratory absorption measurements of WSB in order to adjust A and B for the best fit. The values A = 0.623 and B = 0.41 were found to give the form factor which is closest to reproducing the laboratory data for a dilute mixture of CO₂ in nitrogen at T=296 K. Table 4.2 lists this FASCOD2 form factor in numerical form in addition to the others which have been discussed above.

A principal advantage of the FASCOD2 CO₂ lineshape is that the problem of specifying a turn-on point for sub-Lorentzian behavior has been avoided. A key test of this lineshape is whether it can produce a continuum absorption curve which compares favorably to the other exponential-type fits. We have found the FASCOD2 shape to fit the WSB data slightly better than the best simple exponential form factor with C = 0.5. The difference is slight, but the FASCOD2 lineshape model does appear to be more than adequate to fit the data. A first comparison was made with the simulated CO₂ continuum transmittance for a 5.1 km atmospheric path reported in [26]. The FASCOD2 predictions are displayed in Fig. 4.1 as points on the transmittance curve of Roney et al.²⁶ The comparison reflects a difference of only 1-2 percent between the two models.

Further comparisons are shown in Figs. 4.2 and 4.3. In Fig. 4.2 the stratospheric transmittance data of Smith et al.¹⁹ is reproduced (a) and displayed above a FASCOD2 synthetic spectrum (b) made at AFGL using the new CO₂ continuum model. The agreement appears to be quite good, with FASCOD2 most nearly matching the curve for the lineshape model of Susskind and Mo (curve 2) at the bandhead. Fig. 4.3 shows the 6.4 km (P = 880 mbar, T = 33°C)

path transmittance (a) measured by Hanley et al²⁷ above the corresponding FASCOD2 calculation (b). Again agreement is quite good, indicating that the FASCOD2 CO₂ form factor does give an improved fit to the far wing absorption, at least near the 4.3 μ m bandhead.

TABLE 4.2 COMPARISON OF VARIOUS CO₂ LINESHAPE FORM FACTORS

| DELTA [CM-1] | FASCOD2 | WSB | BURCH | SUSS.,MO | CANN ET AL |
|--------------|----------|----------|----------|----------|------------|
| 2.0 | 0.895189 | 1.000000 | 0.414740 | 0.488393 | 0.811930 |
| 4.0 | 0.580313 | 1.000000 | 0.286610 | 0.355176 | 0.647770 |
| 6.0 | 0.283527 | 0.631284 | 0.208990 | 0.283801 | 0.507540 |
| 8.0 | 0.231923 | 0.466504 | 0.159790 | 0.236701 | 0.391230 |
| 10.0 | 0.201623 | 0.381189 | 0.127360 | 0.202576 | 0.298840 |
| 12.0 | 0.178058 | 0.324358 | 0.105270 | 0.176458 | 0.230360 |
| 14.0 | 0.159098 | 0.282553 | 0.089794 | 0.155722 | 0.185820 |
| 16.0 | 0.143463 | 0.250046 | 0.078712 | 0.138817 | 0.165190 |
| 18.0 | 0.130322 | 0.223839 | 0.070627 | 0.124757 | 0.156520 |
| 20.0 | 0.119111 | 0.202165 | 0.064643 | 0.112875 | 0.148310 |
| 22.0 | 0.109428 | 0.183890 | 0.060164 | 0.102705 | 0.140540 |
| 24.0 | 0.100979 | 0.168248 | 0.056780 | 0.093905 | 0.133190 |
| 26.0 | 0.093543 | 0.154697 | 0.054202 | 0.086222 | 0.126240 |
| 28.0 | 0.086949 | 0.142838 | 0.052221 | 0.079462 | 0.119660 |
| 30.0 | 0.081065 | 0.132373 | 0.050681 | 0.073474 | 0.113440 |
| 32.0 | 0.075783 | 0.123070 | 0.049462 | 0.068138 | 0.107570 |
| 34.0 | 0.071019 | 0.114748 | 0.048472 | 0.063358 | 0.102020 |
| 36.0 | 0.066702 | 0.107264 | 0.047638 | 0.059056 | 0.096774 |
| 38.0 | 0.062774 | 0.100500 | 0.046900 | 0.055168 | 0.091822 |
| 40.0 | 0.059188 | 0.094360 | 0.046213 | 0.051640 | 0.087148 |
| 42.0 | 0.055901 | 0.088766 | 0.045538 | 0.048429 | 0.082736 |
| 44.0 | 0.052881 | 0.083650 | 0.044848 | 0.045495 | 0.078572 |
| 46.0 | 0.050098 | 0.078957 | 0.044120 | 0.042808 | 0.074644 |
| 48.0 | 0.047526 | 0.074639 | 0.043340 | 0.040340 | 0.070939 |
| 50.0 | 0.045144 | 0.070656 | 0.042496 | 0.038068 | 0.067444 |
| 52.0 | 0.042933 | 0.066972 | 0.041585 | 0.035971 | 0.064148 |
| 54.0 | 0.040877 | 0.063558 | 0.040605 | 0.034031 | 0.061040 |
| 56.0 | 0.038960 | 0.060387 | 0.039558 | 0.032233 | 0.058110 |
| 58.0 | 0.037170 | 0.057435 | 0.038451 | 0.030563 | 0.055347 |
| 60.0 | 0.035496 | 0.054683 | 0.037290 | 0.029011 | 0.052743 |
| 62.0 | 0.033928 | 0.052113 | 0.036084 | 0.027564 | 0.050287 |
| 64.0 | 0.032457 | 0.049709 | 0.034844 | 0.026213 | 0.047972 |
| 66.0 | 0.031074 | 0.047456 | 0.033580 | 0.024951 | 0.045789 |
| 68.0 | 0.029774 | 0.045342 | 0.032302 | 0.023770 | 0.043730 |
| 70.0 | 0.028549 | 0.043355 | 0.031021 | 0.022663 | 0.041789 |
| 72.0 | 0.027394 | 0.041487 | 0.029746 | 0.021625 | 0.039958 |
| 74.0 | 0.026303 | 0.039727 | 0.028486 | 0.020649 | 0.038230 |
| 76.0 | 0.025271 | 0.038067 | 0.027248 | 0.019731 | 0.036599 |
| 78.0 | 0.024295 | 0.036500 | 0.026040 | 0.018866 | 0.035059 |
| 80.0 | 0.023371 | 0.035019 | 0.024866 | 0.018052 | 0.033605 |
| 82.0 | 0.022495 | 0.033618 | 0.023732 | 0.017283 | 0.032231 |
| 84.0 | 0.021663 | 0.032292 | 0.022640 | 0.016557 | 0.030933 |
| 86.0 | 0.020873 | 0.031035 | 0.021594 | 0.015870 | 0.029705 |
| 88.0 | 0.020122 | 0.029842 | 0.020595 | 0.015221 | 0.028543 |
| 90.0 | 0.019407 | 0.028710 | 0.019643 | 0.014606 | 0.027443 |

TABLE 4.2 (CONT.)

| DELTA [CM-1] | FASCOD2 | WSB | BURCH | SUSS.,MO | CANN ET AL |
|--------------|----------|----------|----------|----------|------------|
| 92.0 | 0.018727 | 0.027634 | 0.018739 | 0.014023 | 0.026401 |
| 94.0 | 0.018079 | 0.026612 | 0.017883 | 0.013470 | 0.025413 |
| 96.0 | 0.017461 | 0.025638 | 0.017074 | 0.012945 | 0.024477 |
| 98.0 | 0.016871 | 0.024711 | 0.016310 | 0.012446 | 0.023587 |
| 100.0 | 0.016308 | 0.023828 | 0.015591 | 0.011972 | 0.022742 |
| 102.0 | 0.015770 | 0.022986 | 0.014913 | 0.011521 | 0.021939 |
| 104.0 | 0.015255 | 0.022182 | 0.014276 | 0.011092 | 0.021175 |
| 106.0 | 0.014763 | 0.021415 | 0.013677 | 0.010683 | 0.020447 |
| 108.0 | 0.014292 | 0.020682 | 0.013114 | 0.010294 | 0.019754 |
| 110.0 | 0.013841 | 0.019981 | 0.012584 | 0.009922 | 0.019092 |
| 112.0 | 0.013408 | 0.019311 | 0.012087 | 0.009568 | 0.018460 |
| 114.0 | 0.012994 | 0.018670 | 0.011619 | 0.009229 | 0.017857 |
| 116.0 | 0.012596 | 0.018056 | 0.011179 | 0.008906 | 0.017280 |
| 118.0 | 0.012214 | 0.017468 | 0.010765 | 0.008597 | 0.016728 |
| 120.0 | 0.011848 | 0.016905 | 0.010374 | 0.008302 | 0.016199 |
| 122.0 | 0.011496 | 0.016364 | 0.010005 | 0.008019 | 0.015692 |
| 124.0 | 0.011158 | 0.015846 | 0.009656 | 0.007749 | 0.015206 |
| 126.0 | 0.010832 | 0.015348 | 0.009326 | 0.007490 | 0.014739 |
| 128.0 | 0.010519 | 0.014871 | 0.009012 | 0.007241 | 0.014291 |
| 130.0 | 0.010218 | 0.014412 | 0.008714 | 0.007003 | 0.013861 |
| 132.0 | 0.009928 | 0.013971 | 0.008431 | 0.006775 | 0.013447 |
| 134.0 | 0.009649 | 0.013547 | 0.008160 | 0.006557 | 0.013049 |
| 136.0 | 0.009380 | 0.013139 | 0.007901 | 0.006347 | 0.012665 |
| 138.0 | 0.009121 | 0.012747 | 0.007653 | 0.006145 | 0.012297 |
| 140.0 | 0.008871 | 0.012370 | 0.007414 | 0.005951 | 0.011941 |
| 142.0 | 0.008630 | 0.012006 | 0.007185 | 0.005765 | 0.011599 |
| 144.0 | 0.008397 | 0.011657 | 0.006964 | 0.005587 | 0.011270 |
| 146.0 | 0.008172 | 0.011319 | 0.006750 | 0.005415 | 0.010953 |
| 148.0 | 0.007956 | 0.010994 | 0.006543 | 0.005249 | 0.010647 |
| 150.0 | 0.007746 | 0.010681 | 0.006343 | 0.005090 | 0.010353 |
| 152.0 | 0.007544 | 0.010379 | 0.006149 | 0.004937 | 0.010070 |
| 154.0 | 0.007348 | 0.010087 | 0.005960 | 0.004790 | 0.009797 |
| 156.0 | 0.007159 | 0.009806 | 0.005776 | 0.004648 | 0.009535 |
| 158.0 | 0.006976 | 0.009535 | 0.005598 | 0.004511 | 0.009283 |
| 160.0 | 0.006800 | 0.009273 | 0.005424 | 0.004379 | 0.009040 |
| 162.0 | 0.006629 | 0.009019 | 0.005255 | 0.004252 | 0.008807 |
| 164.0 | 0.006463 | 0.008775 | 0.005090 | 0.004129 | 0.008584 |
| 166.0 | 0.006303 | 0.008538 | 0.004929 | 0.004011 | 0.008370 |
| 168.0 | 0.006147 | 0.008310 | 0.004773 | 0.003897 | 0.008164 |
| 170.0 | 0.005997 | 0.008089 | 0.004620 | 0.003787 | 0.007967 |
| 172.0 | 0.005851 | 0.007875 | 0.004472 | 0.003681 | 0.007779 |
| 174.0 | 0.005710 | 0.007668 | 0.004329 | 0.003578 | 0.007599 |
| 176.0 | 0.005573 | 0.007468 | 0.004189 | 0.003479 | 0.007428 |
| 178.0 | 0.005441 | 0.007275 | 0.004053 | 0.003383 | 0.007265 |
| 180.0 | 0.005312 | 0.007087 | 0.003922 | 0.003291 | 0.007109 |
| 182.0 | 0.005187 | 0.006906 | 0.003795 | 0.003201 | 0.006961 |
| 184.0 | 0.005066 | 0.006730 | 0.003672 | 0.003115 | 0.006821 |

TABLE 4.2 (CONT.)

| DELTA [CM-1] | FASCOD2 | WSB | BURCH | SUSS.,MO | CANN ET AL |
|--------------|----------|----------|----------|----------|------------|
| 186.0 | 0.004948 | 0.006560 | 0.003553 | 0.003031 | 0.006689 |
| 188.0 | 0.004834 | 0.006395 | 0.003439 | 0.002950 | 0.006563 |
| 190.0 | 0.004723 | 0.006235 | 0.003329 | 0.002872 | 0.006445 |
| 192.0 | 0.004616 | 0.006080 | 0.003223 | 0.002796 | 0.006334 |
| 194.0 | 0.004511 | 0.005930 | 0.003121 | 0.002723 | 0.006229 |
| 196.0 | 0.004410 | 0.005784 | 0.003024 | 0.002652 | 0.006131 |
| 198.0 | 0.004311 | 0.005642 | 0.002930 | 0.002583 | 0.006040 |
| 200.0 | 0.004215 | 0.005505 | 0.002841 | 0.002517 | 0.005954 |
| 202.0 | 0.004122 | 0.005372 | 0.002755 | 0.002452 | 0.005875 |
| 204.0 | 0.004032 | 0.005243 | 0.002674 | 0.002390 | 0.005801 |
| 206.0 | 0.003943 | 0.005118 | 0.002596 | 0.002329 | 0.005733 |
| 208.0 | 0.003858 | 0.004996 | 0.002522 | 0.002270 | 0.005670 |
| 210.0 | 0.003774 | 0.004878 | 0.002452 | 0.002213 | 0.005613 |
| 212.0 | 0.003693 | 0.004763 | 0.002385 | 0.002158 | 0.005560 |
| 214.0 | 0.003614 | 0.004651 | 0.002322 | 0.002105 | 0.005513 |
| 216.0 | 0.003537 | 0.004543 | 0.002262 | 0.002053 | 0.005469 |
| 218.0 | 0.003463 | 0.004437 | 0.002205 | 0.002002 | 0.005430 |
| 220.0 | 0.003390 | 0.004335 | 0.002151 | 0.001953 | 0.005395 |
| 222.0 | 0.003319 | 0.004236 | 0.002099 | 0.001906 | 0.005364 |
| 224.0 | 0.003250 | 0.004139 | 0.002051 | 0.001860 | 0.005336 |
| 226.0 | 0.003183 | 0.004045 | 0.002005 | 0.001815 | 0.005311 |
| 228.0 | 0.003117 | 0.003953 | 0.001961 | 0.001772 | 0.005290 |
| 230.0 | 0.003053 | 0.003864 | 0.001919 | 0.001729 | 0.005271 |
| 232.0 | 0.002991 | 0.003778 | 0.001880 | 0.001688 | 0.005255 |
| 234.0 | 0.002930 | 0.003693 | 0.001842 | 0.001649 | 0.005241 |
| 236.0 | 0.002871 | 0.003611 | 0.001806 | 0.001610 | 0.005229 |
| 238.0 | 0.002813 | 0.003532 | 0.001771 | 0.001572 | 0.005219 |
| 240.0 | 0.002757 | 0.003454 | 0.001738 | 0.001536 | 0.005210 |
| 242.0 | 0.002702 | 0.003378 | 0.001706 | 0.001500 | 0.005203 |
| 244.0 | 0.002649 | 0.003305 | 0.001675 | 0.001466 | 0.005197 |
| 246.0 | 0.002597 | 0.003233 | 0.001645 | 0.001432 | 0.005192 |
| 248.0 | 0.002546 | 0.003163 | 0.001615 | 0.001399 | 0.005188 |
| 250.0 | 0.002496 | 0.003095 | 0.001586 | 0.001367 | 0.005184 |

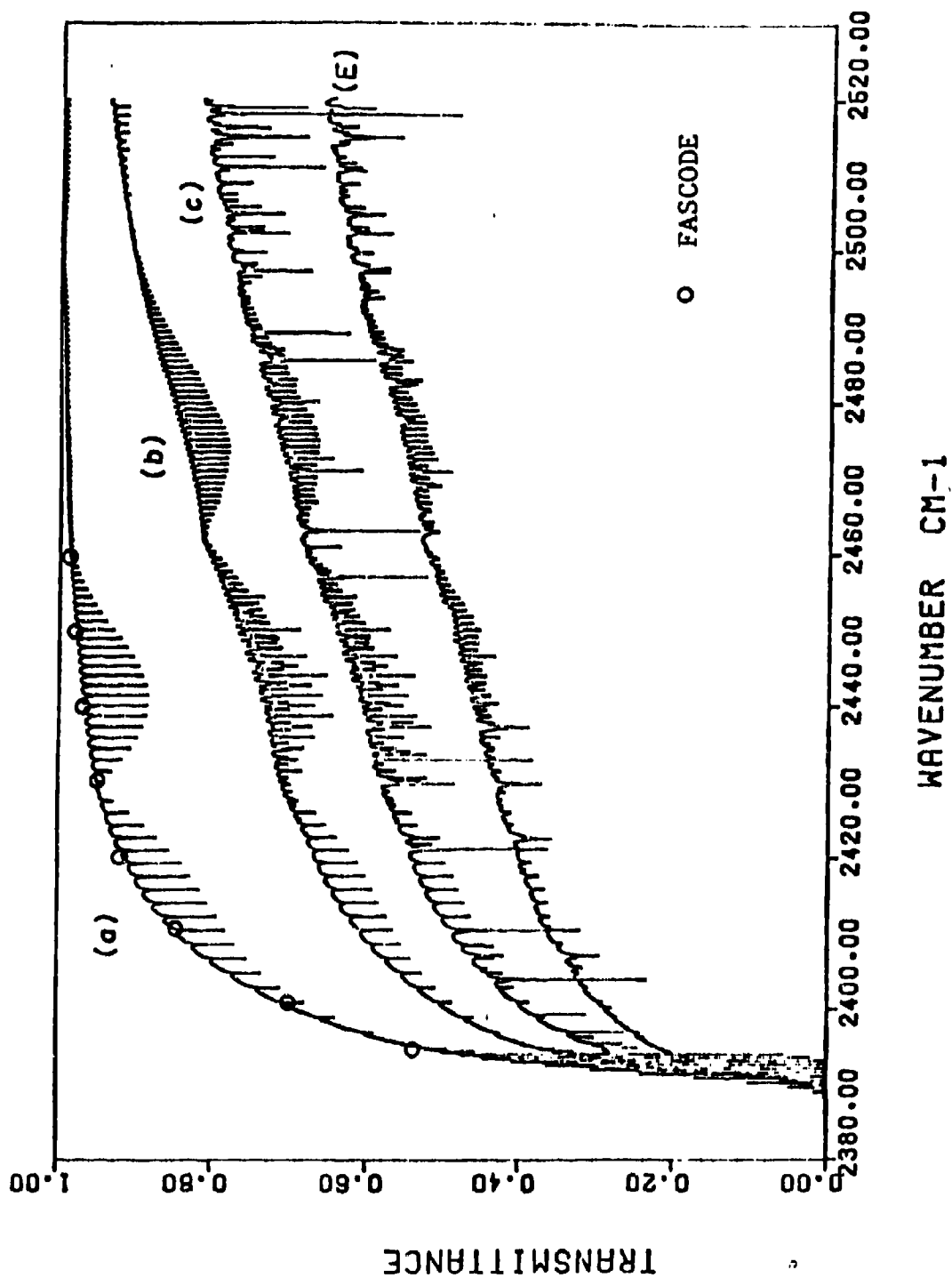


Figure 4.1 Comparison of sample FASCODE CO_2 transmittances to other simulations of (E) NRL Field Spectrum S154. Transmittance curves for (a) CO_2 only, (b) N_2 continuum and N_2O lines added, and (c) water vapor continuum added, are taken from Ref. 18.

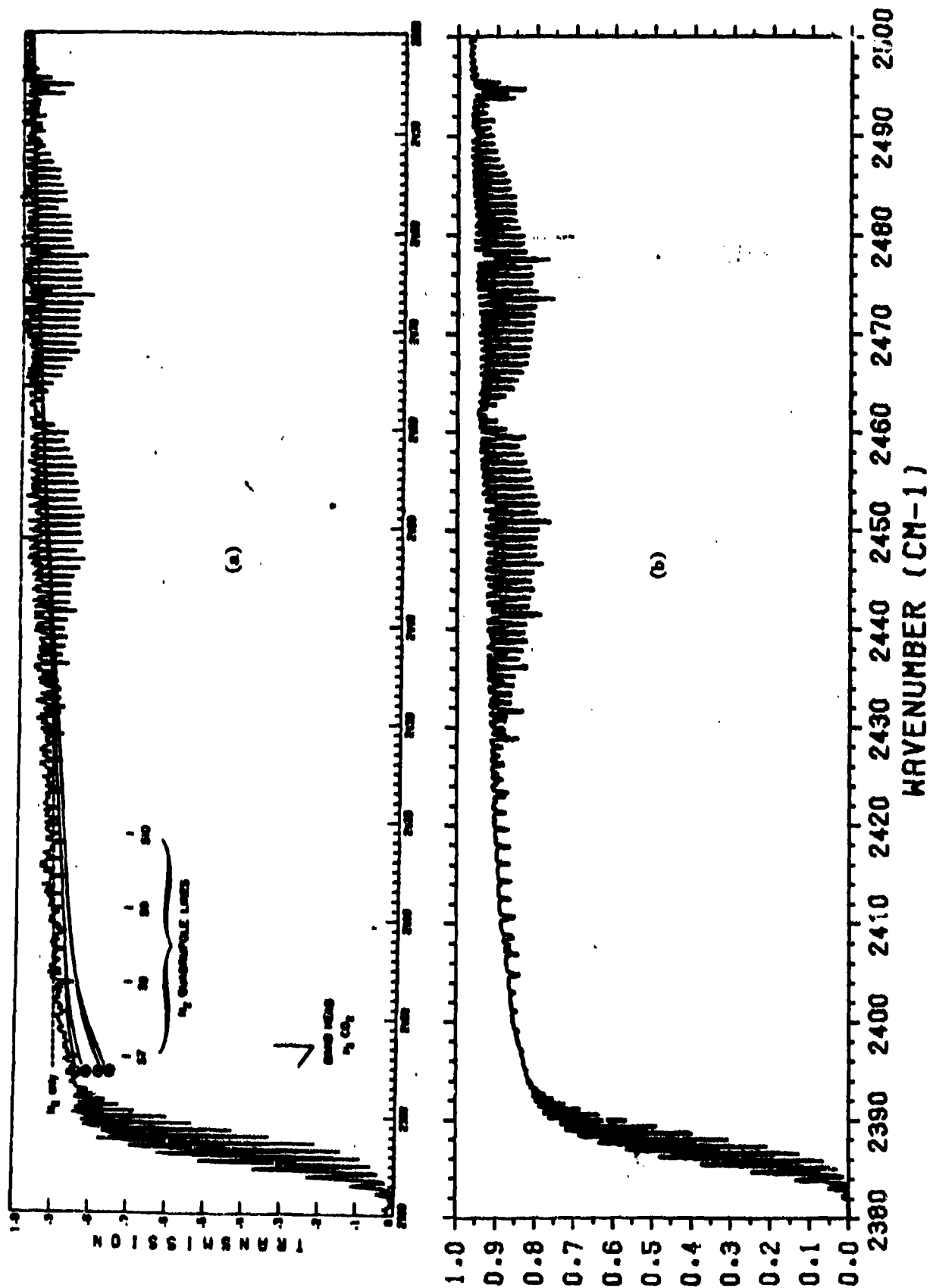


Figure 4.2 Stratospheric transmittance spectrum from balloon observations reproduced from Smith et al. 1969 (a) as compared to (b) and corresponding FASCOB2 spectrum.

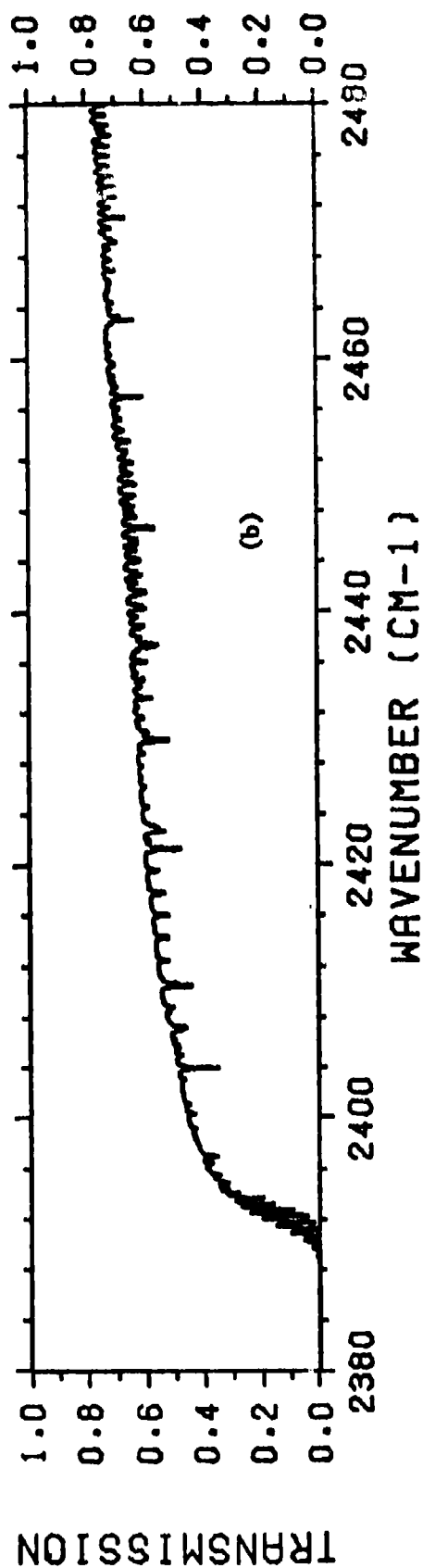
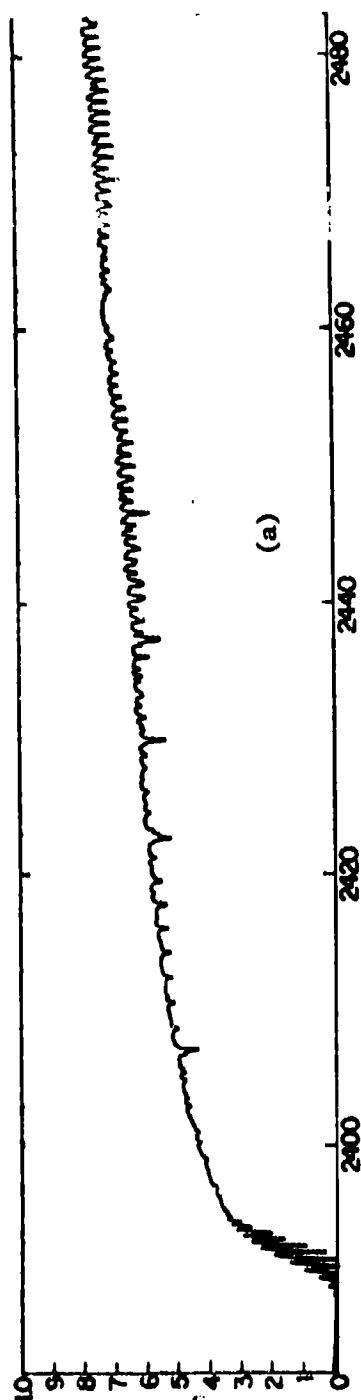


Figure 4.3 Measured atmospheric transmittance over a 6.4 Km path for 8.8 torr H_2O and $33^\circ C$ air temperature as reported by Hanley et al²⁷ (a) as compared to (b) a corresponding FASCOD2 spectrum.

5. LAYERING IN FASCOD

Radiative transfer in FASCOD is calculated in a special medium composed of a number of homogeneous layers that approximate the inhomogeneous atmosphere. The manner in which these layers are chosen and how their radiative properties are obtained effect the accuracy of the radiative transfer. This section discusses this problem by first developing the Curtis-Godson approximation which is a two-parameter, equivalent-line argument for inhomogeneous media. However, such an approximation is cumbersome to execute in the context of FASCOD. An approximation to Curtis-Godson is therefore developed that leads to what is presently done in the various versions of FASCOD. With this information available, the last section makes recommendations for further work.

5.1. Curtis-Godson Approximation: Radiative transfer through inhomogeneous media is always difficult to model in that all the associated spatial integrals must be evaluated numerically on a fine grid. This is operationally cumbersome and computationally expensive. Consequently several approaches have been developed for replacing inhomogeneous media by homogeneous media that are in some way radiatively equivalent. The basis for most of these methods is the Curtis-Godson approximation which is a two-parameter equivalent line argument. This approximation may be developed from several different viewpoints, but the common principle is that certain radiative transfer properties are matched to find the required parameters.

The exact, single-line, spectral optical depth τ_v along some path segment in a given layer for a specific absorber n can be expressed as

$$\tau_v^n = \int_{z_1}^{z_2} S^n(T) f_v^n(T, P) \left(\frac{du^n}{dz} \right) dz . \quad (5.1)$$

Each layer contains N different molecular absorbers designated by a counting index n with total column densities or amounts u_n per unit cross-sectional area given by

$$u_n = \int_{Z_1}^{Z_2} \left(\frac{du_n}{dZ} \right) dZ, \quad (5.2)$$

where Z is the vertical dimension. The derivative includes the density times the secant of the local zenith angle (that may vary with Z) so the path length is accounted for. The line shape function f_ν is normalized such that

$$\int_0^\infty f(\nu) d\nu = 1, \quad (5.3)$$

and S is the line strength. An equivalent homogeneous medium would have an optical depth given by

$$\tau_\nu^n = \bar{S}^n \bar{f}_\nu^n u_n, \quad (5.4)$$

where \bar{f}_ν^n is again normalized as in Eq. (5.3). The spectrally averaged optical depth of expressions (5.1) and (5.4) are equated (which is the same as saying the two approaches are equal in the weak-line limit) which gives the relation

$$\bar{S}^n = \frac{1}{u_n} \int_{Z_1}^{Z_2} S^n(T) \left(\frac{du_n}{dZ} \right) dZ. \quad (5.5)$$

This says that the line strength to use in the homogeneous layer is \bar{S}^n .
 If the radiative transfer is also forced to match in the strong-line
 limit where the line wings dominate, then f_v takes the form

$$f_v \sim \frac{\alpha}{(\nu - \nu_0)^2}, \quad (5.6)$$

where α is the line halfwidth. One therefore obtains the equality that

$$\bar{S}^n \frac{\bar{\alpha}^n u_n}{(\nu - \nu_0)^2} = \frac{1}{(\nu - \nu_0)^2} \int_{z_1}^{z_2} S^n(T) \alpha \frac{du_n}{dz} dz, \quad (5.7)$$

or the equivalent halfwidth is of the form

$$\bar{\alpha}^n = \frac{\int_{z_1}^{z_2} S^n(T) \alpha(T, P) \left(\frac{du_n}{dz} \right) dz}{\int_{z_1}^{z_2} S^n(T) \left(\frac{du_n}{dz} \right) dz}. \quad (5.8)$$

Since α is proportional to $P(T)^{-1/2}$, one obtains

$$\frac{\bar{\alpha}^n}{\alpha_0^n} = \frac{\int_{z_1}^{z_2} S^n(T) \frac{P}{P_0} \left(\frac{T_0}{T} \right)^{1/2} \left(\frac{du_n}{dz} \right) dz}{\bar{S}^n}. \quad (5.9)$$

where α_0 is a reference halfwidth and P_0 and T_0 are the reference pressure
 and temperature, respectively.

The Curtis-Godson approximation replaces any given molecular line in an inhomogeneous medium with a "radiatively equivalent" line in an homogeneous medium that has a single linestrength \bar{S}^n and halfwidth $\bar{\alpha}^n$. The accuracy of this approximation is not easily qualified since it does depend on the specified inhomogeneous structure. To check the accuracy, numerical experiments are usually performed.

The Curtis-Godson approximation says that strength-weighted averages should be used. This would be a complicated and time consuming approach since such averages would have to be performed for each line. The next section develops a further approximation of the Curtis-Godson approach that is much more efficient to execute in FASCOD.

5.2 Present Layering Procedure: If the line strength $S^n(T)$ in any layer between Z_1 and Z_2 in the atmosphere is expanded in a Taylor series about the amount weighted temperature \bar{T} given by

$$\bar{T} = \frac{1}{u_n} \int_{Z_1}^{Z_2} T(z) \left(\frac{du_n}{dz} \right) dz, \quad (5.10)$$

then the linear term is identically zero and Eq. (5.5) gives

$$\bar{S}^n = S^n(\bar{T}) + \left. \frac{\partial^2 S^n}{\partial T^2} \right|_{\bar{T}} \left\{ \frac{1}{u_n} \int_{Z_1}^{Z_2} \frac{(T-\bar{T})^2}{2!} \left(\frac{du_n}{dz} \right) dz + \dots \right\}. \quad (5.11)$$

FASCOD uses $S^n(\bar{T})$ as the layer's line strength and this agrees with the Curtis-Godson approximation to the second-order term shown. For uniformly mixed gases, one has that

$$u_n = C_n u \quad (5.12)$$

where

$$u = \sum_{n=1}^N u_n \quad (5.13)$$

and

$$\sum_{n=1}^N C_n = 1 \quad . \quad (5.14)$$

Therefore the temperature \bar{T} can also be expressed as

$$\bar{T} = \frac{1}{u} \int_{z_1}^{z_2} T(z) \left(\frac{du}{dz} \right) dz \quad , \quad (5.15)$$

which is the mean temperature actually used in FASCOD. The reader should be aware, however, that FASCOD includes nonuniform gases in the sum of Eq.

(5.13) and this is not consistent with the present development. To complete the argument, $S^n(T)$ and $\alpha(T,P)$ are expanded in Taylor series in Eq. (5.8) about \bar{T} and \bar{P} , where \bar{P} is given by

$$\bar{P} = \frac{1}{u_n} \int_{z_1}^{z_2} P(z) \left(\frac{du_n}{dz} \right) dz \quad . \quad (5.16)$$

Again the linear terms will be identically zero and one obtains

$$\alpha^n = \alpha^n(\bar{T}, \bar{P}) + \text{second-order terms} \quad , \quad (5.17)$$

where again the mean pressure \bar{P} used in FASCOD is

$$\bar{P} = \frac{1}{u} \int_{z_1}^{z_2} P(z) \left(\frac{du}{dz} \right) dz \quad (5.18)$$

Using the empirical relationship stated above Eq. (5.9) for α leads to the expression

$$\frac{\bar{\alpha}^n}{\alpha_o^n} = \frac{\bar{P}}{P_o} \left(\frac{T_o}{\bar{T}} \right)^{\frac{1}{2}} + \text{second-order terms} \quad (5.19)$$

that is used in FASCOD. The conclusion is that FASCOD's layer properties are obtained by a Curtis-Godson approximation valid to second order in terms like $(T-\bar{T})^2$ or $(P-\bar{P})^2$ [see Eq. (5.11)]. The use of $S(\bar{T})$ and $\alpha(\bar{T}, \bar{P})$ for each layer in the atmosphere is computationally very efficient since line-by-line averages need not be performed.

Once the radiative properties for each layer are properly obtained, the problem of choosing the layer boundaries must be faced. All the versions of FASCOD used in the work discussed in this report have the layer boundaries specified by the user. The only requirement is that the average line halfwidths cannot vary by more than the ratio of 2 to 1 in adjacent layers. A check on this condition is performed and execution terminated when the requirement is not met. This is inconvenient, and later versions of FASCOD now active at AFGL create more layers and adjust boundaries automatically until the above criterion (or any other value of this ratio set by the user) is satisfied. These later versions of FASCOD also contain a restriction on the temperature difference allowed for adjacent

boundaries. Both of these constraints keep the second-order error terms small in the Curtis-Godson arguments given above. They also play a role in maintaining spectral accuracy. FASCOD has been run for both 32 and 16 layers for a few specific problems and the transmittance and radiance have shown very little change. This says the layering procedure is very conservative and accurate.

5.3. Recommendations For Further Studies: As brought out in the above discussion, the layering in FASCOD is conservative, leads to accurate results, and the radiative properties for each layer are being calculated properly. The one obvious and minor change to be made is that the nonuniformly mixed gases should be handled separately in defining their mean temperature and pressure. Some test runs could be performed to see whether this is an important point in practice.

Since the execution time of FASCOD is dependent on the number of layers used, one would like to know the relationship between the number of layers used and the accuracy of the results. This is not a simple question due to the fact that the code operates with a large number of parameters, all of which can effect the answer. As mentioned above, some experiments have been done on changing the number of layers with a fixed set of parameters. Further numerical experiments should be carried out so the layering procedure, accuracy, and parametric space can be related to develop practical guidelines for the users of FASCOD.

6. CONCLUDING REMARKS

As observed in reading this report, the generic code called FASCOD has been under continuous development by AFGL and Soncraft during the period covered by this contract. The FASCOD versions used varied throughout the work and this was noted in the report. Only those particular sections involved in the present modifications are documented here.

The developments presented here plus those accomplished at AFGL will be combined in the near future into one integrated code with increased capabilities. This integrated code will be released to the public as FASCOD2.

REFERENCES

1. McClatchey, R.A., Benedict, W.S., Clough, S.A., Burch, D.E., Calfee, R.F., Fox, K., Rothman, L.S., and Garing, J.S., "AFCRL Atmospheric Absorption Line Parameters Compilation", AFCRL-TR-73-0096 (1977). AD 782904
2. Rothman, L.S., "AFCL Atmospheric Absorption Line Parameters Compilation: 1980 Version," Applied Optics 20, 791-795 (1981).
3. Rothman, L.S., et al, "AFGL Trace Gas Compilation: 1980 Version," Applied Optics 20, 1323-1328 (1981).
4. Clough, S.A., Kneizys, F.X., and Chetwynd, J.H., "Algorithm for the Calculation of Absorption Coefficient-Pressure Broadened Molecular Transitions", AFGL -TR-77-0164 (1977). AD A047515
5. Smith, H.J.P., Dube, D.J., Gardner, M.E., Clough, S.A., Kneizys, F.X. and Rothman, L.S., "FASCODE - Fast Atmospheric Signature Code (Spectral Transmittance and Radiance)", AFGL-TR-78-0081 (1978). AD A057506
6. Clough, S.A., Kneizys, F.X., Rothman, L.S., and Gallery, W.O., "Atmospheric Spectral Transmittance and Radiance: FASCOD1B", SPIE, vol. 277, p. 152 (1981).
7. Ridgway, W.L., Moose, R.A., and Cogley, A.C., "Atmospheric Transmittance/Radiance Computer Code FASCOD2", AFGL-TR-80-0250, Scientific Report No. 1, Air Force Geophysics Laboratory, Hanscom AFB, Mass. (1980). AD A097593
8. Ridgway, W.L., Moose, R.A., and Cogley, A.C., "Atmospheric Transmittance/Radiance Computer Code FASCOD2", AFGL-TR-81-0357, Scientific Report No. 2, Air Force Geophysics Laboratory, Hanscom AFB, Mass. (1981). AD A113825
9. Kneizys, F.X., Shettle, E.P., Gallery, W.O., Chetwynd, J.H., Abreu, L.W., Selby, J.E.A., Fenn, R.W., and McClatchy, R.A., "Atmospheric Transmittance/Radiance: Computer Code LOWTRAN 5", AFGL-TR-80-0067 (1980). AD A088215
10. Gallery, W.O., Kneizys, F.X., and Clough, S.A., "ATMPATH - Computer Code ATMOSPHERIC PATH", private communication (1979).
11. Degges, T.C. and Smith, H.J.P., "A High Altitude Infrared Radiance Model", AFGL-TR-77-0271 (1977). AD A059242
12. Falcone, V.J., Abreu, L.W., and Shettle, E.P., "Atmospheric Attenuation of Millimeter and Submillimeter Waves: Models and Computer Code", AFGL-TR-79-0253 (1979). AD A084485

REFERENCES (CONT.)

13. Van Vleck, J.H. and Huber, D.L., Rev. Mod. Phys. 49, 939 (1977).
14. Huber, D.L. and Van Vleck, J.H., Rev. Mod. Phys. 38, 187 (1966);
15. Gilles, S.E., "Flow with Coupled Radiative and Vibrational Nonequilibrium in a Diatomic Gas", Air Force Office of Scientific Research, Report 68-1895 (1968).
16. Winters, B.H., Silverman, S., and Benedict, W.S., J. Quant. Spect. Rad. Trans. 4, 527 (1964).
17. Burch, D.E., Gryvnak, D.A., Patty, R.R., and Bartky, C.E., J. Opt. Soc. Am. 59, 267 (1969).
18. K.M. Haught, "High Resolution Atmospheric Transmission Spectra from 5 to 3 μ M", NRL Report 8297, Naval Research Laboratory, Washington, D.C. (1979).
19. Smith, M.A.H., Russell III, J.M., and Park, J.H., "Measurements of Continuum Absorption near 2400 cm^{-1} in the Lower Stratosphere", Preprint Volume, Fourth Conference on Atmospheric Radiation, Toronto, Canada, American Meteorological Society, Boston, Mass. (1981).
20. Clough, S.A. and Kneizys, F.X., private communication (1980).
21. Bernstein, L.S., Robertson, D.C., Conant, J.A., and Sandford, B.P., App. Opt. 18, 2454 (1979).
22. Ben-Aryeh, Y., Weissman, E., and Postan, A., J. Quant. Spect. Rad. Trans. 18, 597 (1977).
23. Postan, A., Weissman, E., and Ben-Aryeh, Y., J. Quant. Spect. Rad. Trans. 18, 617 (1977).
24. Susskind, J. and Mo, I., Preprint Volume, Third Conference on Atmospheric Radiation, Davis, California, American Meteorological Society, Boston, Mass. (1978).
25. Cann, M.W.P., Nicholls, R.W., Roney, P.L., Findlay, F.D., and Blanchard, A., Technical Digest, Topical Meeting on Spectroscopy in Support of Atmospheric Measurements, Sarasota, Florida (1980).
26. Roney, P.L., Findlay, F.D., Blanchard, A., Cann, M.W.P., and Nicholls, R.W., Opt. Lett. 6, 151 (1981).
27. Hanley, S.T., et al., "Atmospheric Transmission Measurements at White Sands Missile Range, August 1978", NRL Report 8422, Naval Research Laboratory, Washington, D.C. (1980).

APPENDIX A: FASCOD2-80 USER'S GUIDE

This appendix documents only those parts of the code that have been changed to include the new geometry routine, the gaseous and aerosol atmospheric models, and the integration and automation of several programs. An example run is also presented and the output format explained.

A.1 Input Card Sequence and Format: In the course of adding the geometry and aerosol routines to FASCOD1, several new control cards were introduced. Some of the original FASCOD1A control cards (same as FASCOD1B) have been consolidated to simplify the input deck structure. The complete input card sequence is listed below. Only the new input parameters are defined here. The user is referred to Ref. [6] for a description of the original FASCOD1 input variables.

Card 1 from FASCOD1 main

XID(I), I = 1, 7
(10A10)

Card 2 from FASCOD1 main

IHIRAC, ILBLF4, ICNTNM, IAERSL, IEMIT, ISCAN, IFILTR, IPLOT,
IATM, MPTS, NPTS (9(4X, I1), 25X, 2I5)

where

IAERSL = 0: aerosol attenuation not included
 = 1: aerosol attenuation included
IATM = 0: ATMPH geometry routines are used
 = 1: ATMPH is not used; layer data is read from TAPE7
 as before

Card 3 from FASCOD1 main

V1, V2, TBOUND, EMISIV (10E10.3)

Card 4 from AERSOL, included only if aerosol attenuation is to be included,
i.e., IAERSL = 1

IHAZE, ISEASN, IVULCN, JP, VIS (4 (4X, I1), 5X, E10.3)

where,

IHAZE = 0 no aerosol attenuation included in the calculation.

- 1 RURAL extinction, 23 km VIS.
- 2 RURAL extinction, 5 km VIS.
- 3 MARITIME extinction, 23 km VIS.
- 4 MARITIME extinction, 5 km VIS.
- 5 URBAN extinction, 5 km VIS.
- 6 TROPOSPHERIC extinction, 50 km VIS.
- 7 USER DEFINED extinction, 23 km VIS. (Read into the program immediately after CARD1. Refer to the main program LOWEM in Appendix A⁵ for the input format of coefficients).
- 8 FOG1 (advection fog) extinction, 0.2 km VIS.
- 9 FOG2 (radiation fog) extinction, 0.5 km VIS.

ISEASN = 0 season determined by the value of MODEL;

SPRING-SUMMER for MODEL = 0, 1, 2, 4, 6, 7
FALL-WINTER for MODEL = 3, 5

- 1 SPRING-SUMMER
- 2 FALL-WINTER

IVULCN = 0, 1 BACKGROUND TROPOSPHERIC profile and extinction

- 2 MODERATE VOLCANIC profile and AGED VOLCANIC extinction
- 3 HIGH VOLCANIC profile and FRESH VOLCANIC extinction
- 4 HIGH VOLCANIC profile and AGED VOLCANIC extinction
- 5 MODERATE VOLCANIC profile and FRESH VOLCANIC extinction

JP = print option parameter, inactive in this version of the code

VIS = meteorological range (km)

(when specified, supercedes default value set by IHAZE).

Cards 5, 6, 7, and the layer boundary cards pertain to ATMPH,

and IATM = 0

Card 5 MODEL, ITYPE, IIN, IMOD, KMAX, RE (515, 5X, F10.4)

where,

MODEL = 0: USER SUPPLIED horizontal path parameters

1: TROPICAL model atmosphere

2: MIDLATITUDE SUMMER

3: MIDLATITUDE WINTER

4. SUBARCTIC SUMMER

5: SUBARCTIC WINTER

6: U.S. STANDARD, 1962

7: USER SUPPLIED atmospheric profile

ITYPE = 1: horizontal path (constant pressure)

2: slant path from H1 to H2

3: slant path from H1 to space (100 km)

IIN = number of boundary altitudes for the FASCOD1 layers (required for ITYPE = 2 OR 3).

IMOD = number of boundary altitudes for USER SUPPLIED atmospheric profile (MODEL 7), default = 34 .

KMAX = number of molecular species for which the amounts are to be calculated, default = 8 .

RE = radius of the earth, defaults: MODEL = 1, RE = 6378.39 km;
MODELS = 2, 3, 6, 7, RE = 6371.23km; MODELS = 4, 5, RE =
6356.91 km.

The formats of control cards 6 and 7 depend on whether the path is horizontal (ITYPE = 1) or slant (ITYPE = 2 or 3) .

For a slant path:

CARD 6: H1, H2, ANGLE, RANGE, BETA, LEN

(5F10.4, 15)

H1 altitude of the observer or receiver (km)

H2 altitude of the other endpoint of the path (km)

ANGLE zenith angle at H1 to H2 (km)

RANGE length of the path from H1 to H2

BETA earth centered angle for the path H1 to H2 (degrees)

LEN = 0, short path; 1, long path through a tangent height.
LEN is used only when ANGLE is GT 90.0 and H1 > H2.
default = 0

Only three of the first five parameters need be specified; for example, H1, H2, ANGLE, or H1, H2, BETA, or H1, ANGLE, RANGE. Refer to the comments in subroutine GMTRY or see Reference[5] for a discussion of allowable combinations of these parameters. Next the boundary altitudes for the FASCODE layers are read in with format (8F10.3).

Card 7: V1, V2 (2F10.3)

V1, V2 initial and final wavenumbers for use in calculating the index of refraction (cm-1)

IF MODEL = 7, the input atmospheric profile is read in after control card 1 in the following format

(HEADER (I), I = 1, 2) (2A10)

A 20 character header describing the profile Z, P, T ((3F10.3)

(DENSITY (K), K = 1, KMAX) (8E10.3):

two cards for each of the IMOD levels giving the altitude (km), pressure (mb), temperature (K), and densities of the molecular species (molecular cm-3) at each level)

For a horizontal path:

CARD 2: Z, P, T, RANGE (DEN(K), K = 1, KMAX) (4F10.3,/, (8E10.3)

Z altitude (km)

P pressure (mb)

T temperature (K)

RANGE path length (km)

DEN(K) density of the K'th molecular species (molecules cm-3)

For MODEL = 1 to 7, only Z and RANGE are used and P, T, and DEN are interpolated.

CARD 3: NOT USED

For model 7, the input model atmosphere is read in after control card 5 as for a slant path.

For model 7 horizontal or slant paths the aerosol amounts must be supplied if aerosol attenuation is to be included, i.e. IAERSL = 1. The following card is repeated once for each atmospheric layer

AWKAER(J)

FORMAT(E10.3)

A.2 Sample Run of FASCOD2-80

The sample run of FASCOD2-80 using the geometry and aerosol options presented here will illustrate the complete input deck structure and provide "standard" output for comparison with the user's version of the code. The complete input file follows.

SCRAF, CM70000, T60.

2710 NAME

ATTACH, TAPE3, LINES2050T02150, ID=NAME, MR=1.

ATTACH, LGO, FASCOD1NAME, ID=NAME, MR=1.

REQUEST, TAPE6, *PF.

MAP, PART.

LDSET, PRESET=INDEF.

LOAD, LGO.

SEGLOAD.

EXECUTE, FASCOD1.

EXIT(U)

CATALOG (TAPE6, FASOUT, ID=NAME)

EOR

FASCODE TREE FASCOD1 - (PATH, HIRAC1, LBLF4, CONTNM, ABSMRG, EMINIT, RADMRG,
, SCANFN, PLOTT, AERSOL, ATMPH)

FASCOD1 GLOBAL MAIN, CONSTS, LINHDR, FILHDR, ABSORB, SCATTR, LBLF4, PROF,
, MISC, OUTPUT

LBLF4 EQUAL RFRPTH

PATH INCLUDE PATH

PATH GLOBAL PATH-SAVE

HIRAC1 INCLUDE HIRAC1, SHAPEL, SHAPEG, VOICON, RDLIN, CNVFN, PANEL, MOLEC,
, QV, CONT, ABSOUT

LBLF4 INCLUDE LBLF4, RDLIN4, CONVF4, MOLEC, QV, SHRINK

CONTNM INCLUDE CONTNM, XINT

ABSMRG INCLUDE ABSMRG, ABSOUT

EMINIT INCLUDE EMINIT, EMIN, EMOUT, BBFN

RADMRG INCLUDE RADMRG, EMIN, EMCUT, BBFN

SCANFN INCLUDE SCANFN, SHAPEG

AERSOL INCLUDE AERSOL

AERSOL GLOBAL ICALL, COEFF, AER-SAVE

PLOTT TREE PLTFAS - (HEADER, AXEST, FPLINE)

AXEST TREE AXES - (AXISL, AXLOG, AX2)

END FASCOD1

EOR

DATA FOR FASCOD2 REPORT, GROUND TO 20 KM, VERTICAL AEROSOLS ON

HI = 1 F4 = 1 CN = 1 AE = 1 EM = 1 SC = 1 FI = 0 PL = 0

2.095E + 03 2.105E + 03 0.000E + 00 0.000E + 00 0.000E + 00

1H = 1 IS = 1 IV = 1 JP = 1 2.30E + 01

| | | | | | | | |
|-------|---|--------|---------|-----|-----|-----|-----|
| 6 | 2 | 21 | | | | | |
| 00.0 | | 20.0 | 00.0 | | | | |
| 0. | | 1. | 2. | 3. | 4. | 5. | 7. |
| 8. | | 9. | 10. | 11. | 12. | 13. | 15. |
| 16. | | 17. | 18. | 19. | 20. | 21. | 23. |
| 2090. | | 2110. | | | | | |
| 1. | | 2095.1 | 2104.95 | 0 | 3 | | |
| -1. | | | | | | | |

EOR

EOF

This file consists of three logical records. The first record contains the job control language necessary to access, load and execute the program. The second record contains the directives used to segment the program during loading to minimize the central memory requirements. The third record contains the input data described earlier. Note, the precise spacing of data is not preserved in the sample input file shown above. The user is referred back to Section A.1 for the exact format of the data. This particular run is in the emission mode using the new geometry and aerosol routines (IATM = 0 and IAERSL = 1). A vertical path from 0 to 20 km was chosen, with layer boundaries every kilometer. The scanning routine is

utilized (ISCAN = 1) while the plotting routine which is machine dependent is not (IPLOT = 0).

The following output file has been truncated to include only output up to the second layer, plus the final layer and the results of the scanning routine. This should be sufficient for a user to verify that his copy of the code is functioning properly. The basic format of the output file remains unchanged. Additional output includes the following:

1. A summary of the AERSOL control parameters as the fourth line of output.
2. A list of the altitude dependent aerosol densities, labelled as "AERSOL PROFILE" on the outfile.
3. A table of aerosol extinction and absorption coefficients in each of the four altitude regions as a function of wavelength. This table is labelled "EXTINCTION AND ABSORPTION COEFFICIENTS", and appears about midway through the output for layer number one.
4. The integrated aerosol amount for each layer, labelled "WKAER=".

MODEL = 6
 ITYPE = 2
 IIN = 21
 IHOD = 34
 KHAX = 8
 RE = 6371.230

SLANT PATH SELECTED, ITYPE = 2

MODEL ATMOSPHERE SELECTED IS: M = 6

U. S. STANDARD, 1962

| I | Z (KM) | P (MB) | T (K) | H2O | CO2 | O3 | N2O | DENSITY | | | |
|----|-----------|-----------|----------|-----------|-----------|-----------|-----------|-------------------|-----------|-----------|-----------|
| | | | | | | | | CH4 (MOL CM-3) | CO | O2 | N2 |
| 1 | 0.000 | 1013.000 | 288.100 | 1.973E+17 | 8.342E+15 | 6.777E+11 | 7.078E+12 | 1.896E+12 | 4.045E+13 | 5.296E+18 | 1.974E+19 |
| 2 | 1.000 | 898.600 | 281.600 | 1.404E+17 | 7.583E+15 | 6.777E+11 | 6.434E+12 | 1.723E+12 | 3.677E+13 | 4.814E+18 | 1.794E+19 |
| 3 | 2.000 | 795.000 | 275.100 | 9.696E+16 | 6.878E+15 | 6.777E+11 | 5.836E+12 | 1.563E+12 | 3.335E+13 | 4.366E+18 | 1.627E+19 |
| 4 | 3.000 | 701.200 | 268.700 | 6.018E+16 | 6.220E+15 | 6.275E+11 | 5.277E+12 | 1.414E+12 | 3.016E+13 | 3.949E+18 | 1.472E+19 |
| 5 | 4.000 | 616.600 | 262.200 | 3.678E+16 | 5.611E+15 | 5.773E+11 | 4.760E+12 | 1.275E+12 | 2.720E+13 | 3.562E+18 | 1.328E+19 |
| 6 | 5.000 | 540.500 | 255.700 | 2.140E+16 | 5.047E+15 | 5.773E+11 | 4.282E+12 | 1.147E+12 | 2.447E+13 | 3.204E+18 | 1.194E+19 |
| 7 | 6.000 | 472.200 | 249.200 | 1.271E+16 | 4.526E+15 | 5.647E+11 | 3.841E+12 | 1.029E+12 | 2.195E+13 | 2.874E+18 | 1.071E+19 |
| 8 | 7.000 | 411.100 | 242.700 | 7.022E+15 | 4.048E+15 | 6.149E+11 | 3.434E+12 | 9.199E+11 | 1.962E+13 | 2.570E+18 | 9.578E+18 |
| 9 | 8.000 | 356.500 | 236.200 | 4.012E+15 | 3.607E+15 | 6.526E+11 | 3.061E+12 | 8.199E+11 | 1.749E+13 | 2.290E+18 | 8.535E+18 |
| 10 | 9.000 | 308.000 | 229.700 | 1.538E+15 | 3.205E+15 | 8.910E+11 | 2.720E+12 | 7.265E+11 | 1.534E+13 | 2.035E+18 | 7.585E+18 |
| 11 | 10.000 | 265.000 | 223.200 | 6.018E+14 | 2.839E+15 | 1.129E+12 | 2.408E+12 | 6.451E+11 | 1.376E+13 | 1.803E+18 | 6.717E+18 |
| 12 | 11.000 | 227.000 | 216.800 | 2.742E+14 | 2.73E+15 | 1.631E+12 | 2.124E+12 | 5.689E+11 | 1.214E+13 | 1.589E+18 | 5.924E+18 |
| 13 | 12.000 | 194.000 | 216.600 | 1.237E+14 | 2.141E+15 | 2.008E+12 | 1.817E+12 | 4.867E+11 | 1.038E+13 | 1.359E+18 | 5.067E+18 |
| 14 | 13.000 | 165.800 | 216.600 | 6.018E+13 | 1.830E+15 | 2.133E+12 | 1.553E+12 | 4.160E+11 | 8.874E+12 | 1.162E+18 | 4.331E+18 |
| 15 | 14.000 | 141.700 | 216.600 | 2.809E+13 | 1.564E+15 | 2.384E+12 | 1.327E+12 | 3.555E+11 | 7.584E+12 | 9.930E+17 | 3.701E+18 |
| 16 | 15.000 | 121.100 | 216.600 | 2.407E+13 | 1.337E+15 | 2.635E+12 | 1.134E+12 | 3.038E+11 | 6.481E+12 | 8.486E+17 | 3.163E+18 |
| 17 | 16.000 | 103.500 | 216.600 | 2.040E+13 | 1.142E+15 | 3.012E+12 | 9.694E+11 | 2.597E+11 | 5.539E+12 | 7.253E+17 | 2.704E+18 |
| 18 | 17.000 | 88.500 | 216.600 | 1.739E+13 | 9.769E+14 | 3.514E+12 | 8.289E+11 | 2.220E+11 | 4.737E+12 | 6.202E+17 | 2.312E+18 |

| | | | | | | | | | | | |
|----|-----------|--------|---------|-----------|-----------|-----------|-----------|-----------|-----------|-----------|-----------|
| 19 | 18.000 | 75.650 | 216.600 | 1.471E+13 | 8.351E+14 | 4.016E+12 | 7.085E+11 | 1.898E+11 | 4.049E+12 | 5.301E+17 | 1.978E+18 |
| 20 | 19.000 | 64.670 | 216.600 | 1.471E+13 | 7.139E+14 | 4.392E+12 | 6.057E+11 | 1.622E+11 | 3.461E+12 | 4.535E+17 | 1.409E+18 |
| 21 | 20.000 | 55.290 | 216.600 | 1.471E+13 | 6.103E+14 | 4.769E+12 | 5.178E+11 | 1.387E+11 | 2.959E+12 | 3.875E+17 | 1.444E+18 |
| 22 | 21.000 | 47.290 | 217.600 | 1.605E+13 | 5.196E+14 | 4.769E+12 | 4.409E+11 | 1.181E+11 | 2.519E+12 | 3.299E+17 | 1.230E+18 |
| 23 | 22.000 | 40.470 | 218.600 | 1.739E+13 | 4.426E+14 | 4.894E+12 | 3.756E+11 | 1.006E+11 | 2.146E+12 | 2.810E+17 | 1.047E+18 |
| 24 | 23.000 | 34.670 | 219.600 | 1.906E+13 | 3.775E+14 | 4.769E+12 | 3.203E+11 | 8.579E+10 | 1.830E+12 | 2.396E+17 | 8.932E+17 |
| 25 | 24.000 | 29.720 | 220.600 | 2.041E+13 | 3.221E+14 | 4.518E+12 | 2.733E+11 | 7.321E+10 | 1.562E+12 | 2.045E+17 | 7.622E+17 |
| 26 | 25.000 | 25.490 | 221.600 | 2.207E+13 | 2.750E+14 | 4.267E+12 | 2.333E+11 | 6.250E+10 | 1.333E+12 | 1.746E+17 | 6.508E+17 |
| 27 | 30.000 | 11.970 | 226.500 | 1.271E+13 | 1.264E+14 | 2.510E+12 | 1.072E+11 | 2.872E+10 | 6.126E+11 | 8.021E+16 | 2.990E+17 |
| 28 | 35.000 | 5.746 | 236.500 | 5.350E+12 | 5.809E+13 | 1.380E+12 | 4.929E+10 | 1.320E+10 | 2.816E+11 | 3.688E+16 | 1.375E+17 |
| 29 | 40.000 | 2.671 | 253.400 | 2.240E+12 | 2.709E+13 | 6.149E+11 | 2.298E+10 | 6.156E+09 | 1.313E+11 | 1.720E+16 | 6.410E+16 |
| 30 | 45.000 | 1.491 | 264.200 | 1.070E+12 | 1.349E+13 | 2.133E+11 | 1.145E+10 | 3.067E+09 | 6.542E+10 | 8.566E+15 | 3.193E+16 |
| 31 | 50.000 | .798 | 270.600 | 4.012E+11 | 7.049E+12 | 5.020E+10 | 5.961E+09 | 1.602E+09 | 3.413E+10 | 4.475E+15 | 1.668E+16 |
| 32 | 70.000 | .055 | 219.700 | 5.015E+09 | 6.007E+11 | 1.079E+09 | 5.097E+08 | 1.365E+08 | 2.913E+09 | 3.814E+14 | 1.422E+15 |
| 33 | 100.000 | .000 | 210.000 | 3.344E+07 | 3.425E+09 | 5.396E+05 | 2.906E+06 | 7.784E+05 | 1.660E+07 | 2.174E+12 | 8.104E+12 |
| 34 | 99999.000 | 0.000 | 190.000 | 0. | 0. | 0. | 0. | 0. | 0. | 0. | 0. |

CONTROL CARD 2: SLANT PATH PARAMETERS

| | | |
|-------|---|------------|
| H1 | = | 0.0000 KM |
| H2 | = | 20.0000 KM |
| ANGLE | = | 0.0000 DEG |
| RANGE | = | 0.0000 KM |
| BETA | = | 0.0000 DEG |
| LEN | = | 0 |

BOUNDARY ALTITUDES FOR FASCOD1 LAYERS

| I | Z (KM) |
|----|--------|
| 1 | 0.0000 |
| 2 | 1.0000 |
| 3 | 2.0000 |
| 4 | 3.0000 |
| 5 | 4.0000 |
| 6 | 5.0000 |
| 7 | 6.0000 |
| 8 | 7.0000 |
| 9 | 8.0000 |
| 10 | 9.0000 |

11 10.0000
12 11.0000
13 12.0000
14 13.0000
15 14.0000
16 15.0000
17 16.0000
18 17.0000
19 18.0000
20 19.0000
21 20.0000

CONTROL CARD 3

V1 = 2090.000 CM-1
V2 = 2110.000 CM-1
VBAR = 2100.000 CM-1

IMMERGED ATMOSPHERIC PROFILE: MODEL ATMOSPHERE PLUS FASCODI LAYER BOUNDARIES

THIS PROFILE IS THE INPUT ATMOSPHERE TO THE GEOMETRY CALCULATION

| I | Z (KM) | P (MB) | T (K) | REFRACT INDEX-1 #1.0E+6 | H2O | CO2 | O3 | DENSITY N2O (MOL CM-3) | CD | CR4 | CD | N2 |
|----|-----------|-----------|----------|-------------------------------|-----------|-----------|-----------|------------------------------|-----------|-----------|-----------|-----------|
| 1 | 0.000 | 1013.000 | 288.100 | 272.098 | 1.973E+17 | 8.342E+15 | 6.777E+11 | 7.078E+12 | 1.896E+12 | 4.045E+13 | 5.296E+18 | 1.974E+17 |
| 2 | 1.000 | 898.600 | 281.600 | 247.012 | 1.404E+17 | 7.583E+15 | 6.777E+11 | 6.434E+12 | 1.723E+12 | 3.677E+13 | 4.814E+18 | 1.794E+19 |
| 3 | 2.000 | 793.000 | 275.100 | 223.751 | 9.696E+16 | 6.878E+15 | 6.777E+11 | 5.836E+12 | 1.563E+12 | 3.335E+13 | 4.366E+18 | 1.627E+19 |
| 4 | 3.000 | 701.200 | 268.700 | 202.099 | 6.018E+16 | 6.220E+15 | 6.275E+11 | 5.277E+12 | 1.414E+12 | 3.016E+13 | 3.949E+18 | 1.472E+19 |
| 5 | 4.000 | 616.600 | 262.200 | 182.151 | 3.678E+16 | 5.611E+15 | 5.773E+11 | 4.760E+12 | 1.275E+12 | 2.720E+13 | 3.542E+18 | 1.325E+19 |
| 6 | 5.000 | 540.500 | 255.700 | 163.748 | 2.140E+16 | 5.047E+15 | 5.773E+11 | 4.282E+12 | 1.147E+12 | 2.447E+13 | 3.204E+18 | 1.194E+19 |
| 7 | 6.000 | 472.200 | 249.200 | 146.797 | 1.271E+16 | 4.526E+15 | 5.647E+11 | 3.841E+12 | 1.029E+12 | 2.195E+13 | 2.874E+18 | 1.071E+19 |
| 8 | 7.000 | 411.100 | 242.700 | 131.232 | 7.022E+15 | 4.048E+15 | 6.149E+11 | 3.434E+12 | 9.199E+11 | 1.962E+13 | 2.570E+18 | 9.578E+18 |
| 9 | 8.000 | 356.500 | 236.200 | 116.938 | 4.012E+15 | 3.607E+15 | 6.523E+11 | 3.061E+12 | 8.199E+11 | 1.749E+13 | 2.290E+18 | 8.536E+18 |
| 10 | 9.000 | 308.000 | 229.700 | 103.891 | 1.538E+15 | 3.205E+15 | 8.910E+11 | 2.720E+12 | 7.285E+11 | 1.554E+13 | 2.035E+18 | 7.535E+18 |
| 11 | 10.000 | 265.000 | 223.200 | 91.991 | 6.018E+14 | 2.839E+15 | 1.129E+12 | 2.408E+12 | 6.451E+11 | 1.376E+13 | 1.802E+18 | 6.717E+18 |
| 12 | 11.000 | 227.000 | 216.800 | 81.126 | 2.742E+14 | 2.503E+15 | 1.631E+12 | 2.124E+12 | 5.689E+11 | 1.214E+13 | 1.509E+18 | 5.924E+18 |
| 13 | 12.000 | 194.000 | 216.600 | 69.397 | 1.237E+14 | 2.141E+15 | 2.008E+12 | 1.817E+12 | 4.867E+11 | 1.038E+12 | 1.309E+18 | 5.087E+18 |
| 14 | 13.000 | 165.800 | 216.600 | 59.309 | 6.018E+13 | 1.830E+15 | 2.133E+12 | 1.553E+12 | 4.140E+11 | 8.874E+11 | 1.162E+18 | 4.331E+18 |
| 15 | 14.000 | 141.700 | 216.600 | 50.688 | 2.809E+13 | 1.564E+15 | 2.384E+12 | 1.327E+12 | 3.555E+11 | 7.594E+11 | 9.930E+17 | 3.701E+18 |

| | | | | | | | | | | | | |
|----|-----------|---------|---------|--------|-----------|-----------|-----------|-----------|-----------|-----------|-----------|-----------|
| 16 | 15.000 | 121.100 | 216.600 | 43.319 | 2.407E+13 | 1.337E+13 | 2.635E+12 | 1.134E+12 | 3.038E+11 | 6.481E+12 | 8.486E+17 | 3.163E+18 |
| 17 | 16.000 | 103.500 | 216.600 | 37.024 | 2.040E+13 | 1.142E+13 | 3.012E+12 | 9.494E+11 | 2.597E+11 | 5.539E+12 | 7.253E+17 | 2.704E+18 |
| 18 | 17.000 | 88.500 | 216.600 | 31.658 | 1.739E+13 | 9.769E+12 | 3.514E+12 | 8.289E+11 | 2.220E+11 | 4.737E+12 | 6.202E+17 | 2.312E+18 |
| 19 | 18.000 | 75.650 | 216.600 | 27.061 | 1.471E+13 | 8.351E+12 | 4.014E+12 | 7.095E+11 | 1.998E+11 | 4.049E+12 | 5.301E+17 | 1.976E+18 |
| 20 | 19.000 | 64.670 | 216.600 | 23.133 | 1.471E+13 | 7.139E+12 | 4.392E+12 | 6.057E+11 | 1.622E+11 | 3.461E+12 | 4.532E+17 | 1.689E+18 |
| 21 | 20.000 | 53.290 | 216.600 | 19.778 | 1.471E+13 | 6.103E+12 | 4.769E+12 | 5.178E+11 | 1.387E+11 | 2.959E+12 | 3.875E+17 | 1.444E+18 |
| 22 | 21.000 | 47.290 | 217.600 | 16.839 | 1.605E+13 | 5.196E+12 | 4.769E+12 | 4.409E+11 | 1.181E+11 | 2.519E+12 | 3.299E+17 | 1.230E+18 |
| 23 | 22.000 | 40.470 | 218.600 | 14.344 | 1.739E+13 | 4.426E+12 | 4.894E+12 | 3.756E+11 | 1.006E+11 | 2.146E+12 | 2.810E+17 | 1.047E+18 |
| 24 | 23.000 | 34.670 | 219.600 | 12.233 | 1.906E+13 | 3.775E+12 | 4.769E+12 | 3.203E+11 | 8.579E+10 | 1.830E+12 | 2.396E+17 | 8.932E+17 |
| 25 | 24.000 | 29.720 | 220.600 | 10.439 | 2.040E+13 | 3.221E+12 | 4.518E+12 | 2.733E+11 | 7.321E+10 | 1.562E+12 | 2.045E+17 | 7.622E+17 |
| 26 | 25.000 | 25.490 | 221.600 | 8.912 | 2.207E+13 | 2.750E+12 | 4.267E+12 | 2.333E+11 | 6.250E+10 | 1.333E+12 | 1.746E+17 | 6.503E+17 |
| 27 | 30.000 | 11.970 | 226.500 | 4.095 | 1.271E+13 | 1.264E+12 | 2.510E+12 | 1.072E+11 | 2.872E+10 | 6.126E+11 | 8.021E+16 | 2.990E+17 |
| 28 | 35.000 | 5.746 | 236.500 | 1.882 | 5.350E+12 | 5.809E+13 | 1.380E+12 | 4.929E+10 | 1.320E+10 | 2.816E+11 | 3.488E+16 | 1.375E+17 |
| 29 | 40.000 | 2.871 | 253.400 | .878 | 2.240E+12 | 2.709E+13 | 6.149E+11 | 2.298E+10 | 6.156E+09 | 1.313E+11 | 1.720E+16 | 6.410E+16 |
| 30 | 45.000 | 1.491 | 264.200 | .437 | 1.070E+12 | 1.349E+13 | 2.133E+11 | 1.145E+10 | 3.067E+09 | 6.542E+10 | 8.566E+15 | 3.193E+16 |
| 31 | 50.000 | .798 | 270.600 | .228 | 4.012E+11 | 7.049E+12 | 5.020E+10 | 5.981E+09 | 1.602E+09 | 3.418E+10 | 4.475E+15 | 1.669E+16 |
| 32 | 70.000 | .053 | 219.700 | .019 | 5.015E+09 | 6.007E+11 | 1.079E+09 | 5.097E+08 | 1.365E+08 | 2.913E+09 | 3.814E+14 | 1.422E+15 |
| 33 | 100.000 | .000 | 210.000 | .000 | 3.344E+07 | 3.425E+09 | 5.396E+05 | 2.906E+06 | 7.784E+06 | 1.660E+07 | 2.174E+12 | 8.104E+12 |
| 34 | 99999.000 | 0.000 | 190.000 | 0.000 | 0.000 | 0.000 | 0.000 | 0.000 | 0.000 | 0.000 | 0.000 | 0.000 |

ISLAND PATH PARAMETERS AFTER INPUT PROCESSING

H1 = 0.000 KM
 H2 = 20.000 KM
 ANGLE = 0.000 DEG
 HMIN = 0.000 KM
 LEN = 0

CALCULATION OF THE REFRACTED PATH THROUGH THE ATMOSPHERE

| I | ALTITUDE FROM (KM) | TO (KM) | THETA (DEG) | DRANGE (KM) | RANGE (KM) | DBETA (DEG) | BETA (DEG) | PHI (DEG) | DBEND (DEG) | BENDING (DEG) | PBAR (MB) | TBAR (K) | RHOBAR (MOL CM-2) |
|---|--------------------------|------------|----------------|----------------|---------------|----------------|---------------|--------------|----------------|------------------|--------------|-------------|----------------------|
|---|--------------------------|------------|----------------|----------------|---------------|----------------|---------------|--------------|----------------|------------------|--------------|-------------|----------------------|

| | | | | | | | | | | | |
|---|----|--------|--------|-----------|-----------|-----------|-----------|-----------|-----------|-----------|-----------|
| 0 | 9 | 8.000 | 9.000 | 2.590E+20 | 3.402E+20 | 7.656E+16 | 2.387E+17 | 7.733E+16 | 1.650E+18 | 2.160E+23 | 8.051E+23 |
| 0 | 10 | 9.000 | 10.000 | 9.977E+19 | 3.018E+20 | 1.095E+17 | 2.581E+17 | 6.860E+16 | 1.463E+18 | 1.916E+23 | 7.147E+23 |
| 0 | 11 | 10.000 | 11.000 | 4.168E+19 | 2.667E+20 | 1.365E+17 | 2.263E+17 | 6.062E+16 | 1.293E+18 | 1.693E+23 | 6.312E+23 |
| 0 | 12 | 11.000 | 12.000 | 1.891E+19 | 2.317E+20 | 1.813E+17 | 1.967E+17 | 5.267E+16 | 1.124E+18 | 1.471E+23 | 5.484E+23 |
| 0 | 13 | 12.000 | 13.000 | 8.316E+18 | 1.951E+20 | 2.070E+17 | 1.582E+17 | 4.504E+16 | 9.607E+17 | 1.258E+23 | 4.689E+23 |
| 0 | 14 | 13.000 | 14.000 | 4.212E+19 | 1.694E+20 | 2.256E+17 | 1.437E+17 | 3.850E+16 | 8.212E+17 | 1.075E+23 | 4.008E+23 |
| 0 | 15 | 14.000 | 15.000 | 2.603E+19 | 1.448E+20 | 2.507E+17 | 1.228E+17 | 3.290E+16 | 7.018E+17 | 9.199E+22 | 3.425E+23 |
| 0 | 16 | 15.000 | 16.000 | 2.218E+19 | 1.237E+20 | 2.819E+17 | 1.050E+17 | 2.812E+16 | 5.992E+17 | 7.853E+22 | 2.928E+23 |
| 0 | 17 | 16.000 | 17.000 | 1.885E+19 | 1.057E+20 | 3.257E+17 | 8.973E+16 | 2.404E+16 | 5.120E+17 | 6.714E+22 | 2.503E+23 |
| 0 | 18 | 17.000 | 18.000 | 1.601E+19 | 9.041E+19 | 3.759E+17 | 7.671E+16 | 2.055E+16 | 4.394E+17 | 5.740E+22 | 2.140E+23 |
| 0 | 19 | 18.000 | 19.000 | 1.471E+19 | 7.729E+19 | 4.201E+17 | 6.558E+16 | 1.756E+16 | 3.747E+17 | 4.906E+22 | 1.829E+23 |
| 0 | 20 | 19.000 | 20.000 | 1.471E+19 | 6.607E+19 | 4.578E+17 | 5.606E+16 | 1.501E+16 | 3.203E+17 | 4.195E+22 | 1.563E+23 |

IF FINAL SET OF LAYERS FOR INPUT TO FASCODI
IF THE RATIO OF THE THICKNESSES OF TWO ADJACENT LAYERS IS GREATER THAN 10.0,
THEN MERGE THESE LAYERS

| L | LAYER BOUNDARIES | | ICNTRL | PBAR (MB) | TBAR (K) | AIR | H2O | CO2 | INTEGRATED AMOUNTS | | | | D2 | N2 |
|---|------------------|------------|--------|--------------|-------------|----------|----------|----------|--------------------|-------------------|----------|----------|----------|----------|
| | FROM (KM) | TO (KM) | | | | | | | O3 | N2O (MOL CM-2) | CO | CH4 | | |
| 1 | 0.000 | 1.000 | 1 | 955.58 | 284.89 | 2.43E+24 | 1.67E+22 | 7.96E+20 | 6.79E+16 | 6.75E+17 | 1.81E+17 | 3.86E+18 | 5.05E+23 | 1.83E+24 |
| 2 | 1.000 | 2.000 | 1 | 846.60 | 276.39 | 2.20E+24 | 1.17E+22 | 7.22E+20 | 6.78E+16 | 6.13E+17 | 1.64E+17 | 3.50E+18 | 4.59E+23 | 1.71E+24 |
| 3 | 2.000 | 3.000 | 1 | 747.92 | 271.94 | 1.99E+24 | 7.71E+21 | 6.54E+20 | 6.52E+16 | 5.55E+17 | 1.49E+17 | 3.17E+18 | 4.15E+23 | 1.55E+24 |
| 4 | 3.000 | 4.000 | 1 | 638.73 | 265.49 | 1.80E+24 | 4.75E+21 | 5.91E+20 | 6.02E+16 | 5.01E+17 | 1.34E+17 | 2.87E+18 | 3.75E+23 | 1.40E+24 |
| 5 | 4.000 | 5.000 | 1 | 578.39 | 258.99 | 1.62E+24 | 2.84E+21 | 5.32E+20 | 5.77E+16 | 4.52E+17 | 1.21E+17 | 2.58E+18 | 3.38E+23 | 1.26E+24 |
| 6 | 5.000 | 6.000 | 1 | 506.20 | 252.50 | 1.45E+24 | 1.67E+21 | 4.78E+20 | 5.71E+16 | 4.06E+17 | 1.09E+17 | 2.32E+18 | 3.04E+23 | 1.13E+24 |
| 7 | 6.000 | 7.000 | 1 | 441.52 | 246.00 | 1.30E+24 | 9.59E+20 | 4.28E+20 | 5.89E+16 | 3.63E+17 | 9.73E+16 | 2.09E+18 | 2.72E+23 | 1.01E+24 |

| | | | | | | | | | | | | | | |
|----|--------|--------|---|--------|--------|----------|----------|----------|----------|----------|----------|----------|----------|----------|
| 8 | 7.000 | 8.000 | 1 | 383.68 | 239.50 | 1.16E+24 | 5.38E+20 | 3.82E+20 | 6.34E+16 | 3.24E+17 | 8.69E+16 | 1.95E+10 | 2.43E+23 | 9.05E+23 |
| 9 | 8.000 | 9.000 | 1 | 332.14 | 233.00 | 1.03E+24 | 2.58E+20 | 3.40E+20 | 7.66E+16 | 2.89E+17 | 7.73E+16 | 1.65E+18 | 2.16E+23 | 8.05E+23 |
| 10 | 9.000 | 10.000 | 1 | 286.40 | 226.50 | 9.14E+23 | 9.98E+19 | 3.02E+20 | 1.01E+17 | 2.56E+17 | 6.84E+16 | 1.46E+18 | 1.92E+23 | 7.14E+23 |
| 11 | 10.000 | 11.000 | 1 | 245.91 | 220.05 | 8.08E+23 | 4.17E+19 | 2.67E+20 | 1.36E+17 | 2.26E+17 | 6.04E+16 | 1.29E+18 | 1.69E+23 | 6.31E+23 |
| 12 | 11.000 | 12.000 | 1 | 210.50 | 216.70 | 7.02E+23 | 1.89E+19 | 2.32E+20 | 1.81E+17 | 1.97E+17 | 5.27E+16 | 1.12E+19 | 1.47E+23 | 5.48E+23 |
| 13 | 12.000 | 13.000 | 1 | 179.90 | 216.60 | 6.00E+23 | 8.82E+18 | 1.98E+20 | 2.07E+17 | 1.68E+17 | 4.50E+16 | 9.61E+17 | 1.26E+23 | 4.69E+23 |
| 14 | 13.000 | 14.000 | 1 | 153.75 | 216.60 | 5.13E+23 | 4.21E+18 | 1.69E+20 | 2.26E+17 | 1.44E+17 | 3.35E+16 | 8.21E+17 | 1.03E+23 | 4.01E+23 |
| 15 | 14.000 | 15.000 | 1 | 131.40 | 216.60 | 4.38E+23 | 2.60E+18 | 1.45E+20 | 2.51E+17 | 1.23E+17 | 3.29E+16 | 7.02E+17 | 9.19E+22 | 3.42E+23 |
| 16 | 15.000 | 16.000 | 1 | 112.30 | 216.60 | 3.75E+23 | 2.22E+18 | 1.24E+20 | 2.82E+17 | 1.05E+17 | 2.81E+16 | 6.00E+17 | 7.85E+22 | 2.93E+23 |
| 17 | 16.000 | 17.000 | 1 | 96.00 | 216.60 | 3.20E+23 | 1.89E+18 | 1.06E+20 | 3.26E+17 | 8.97E+16 | 2.40E+16 | 5.13E+17 | 6.71E+22 | 2.50E+23 |
| 18 | 17.000 | 18.000 | 1 | 82.07 | 216.60 | 2.74E+23 | 1.60E+18 | 9.04E+19 | 3.76E+17 | 7.67E+16 | 2.05E+16 | 4.38E+17 | 5.74E+22 | 2.14E+23 |
| 19 | 18.000 | 19.000 | 1 | 70.16 | 216.60 | 2.34E+23 | 1.47E+18 | 7.73E+19 | 4.20E+17 | 6.56E+16 | 1.76E+16 | 3.75E+17 | 4.91E+22 | 1.33E+23 |
| 20 | 19.000 | 20.000 | 1 | 59.98 | 216.60 | 2.00E+23 | 1.47E+18 | 6.61E+19 | 4.58E+17 | 5.61E+16 | 1.50E+16 | 3.20E+17 | 4.19E+22 | 1.56E+23 |

AVERAGE RELATIVE HUMIDITY FROM 0 TO 2 KM IS .396E+02

0 V1(CM-1) = 2095.0000
 0 V2(CM-1) = 2105.0000
 0 TBOUND = 0.0000

BOUNDARY EMISSIVITY = 0.00000

LINE FILE INFORMATION

0 ONLINE PARAMETERS TAPE IS ONLY SOURCE FOR FASCOD1

BCDMRG1 79/11/12. 10.38.40.

H20 = 65
 C02 = 333
 C03 = 402
 N20 = 0
 C01 = 23
 C04 = 0
 C02 = 0

0 LOWEST LINE = 2090.042

HIGHEST LINE = 2109.990

TOTAL NUMBER OF LINES = 823

DATA FOR FASCOD2 REPORT, GROUND TO 20 KM, VERTICAL AEROSOLS ON

0 LAYER = 1
 0 PRESS(H3) = 955.58254
 0 TEMP(K) = 284.89
 0 SECANT = 1.00000

H20 = 1.672E+22
 C02 = 7.956E+20
 O3 = 6.777E+16
 N2O = 6.751E+17
 CO = 1.808E+17
 CH4 = 3.858E+18
 O2 = 5.051E+23

N2 = 1.883E+24
 0 WKAER = .12855E+00
 0 SELF BROADENING FACTOR FOR H2O IS 1.02781
 0 COMPUTED DV BEFORE MODIFICATION = .02471832

TYPE OF PATH = 1
 RATIO OF PREVIOUS DV TO CURRENT DV = 0.0000

TYPE OF MERGE 99
 0 DV FOR THE LAYER .02470000

ICH 1 6 10 15
 EXTINCTION AND ABSORPTION COEFFICIENTS

| | | | | | | | | |
|---------|---------|--------|---------|--------|---------|---------|---------|--------|
| .2000 | 2.09397 | .65394 | 2.21519 | .65000 | 1.48471 | 0.00000 | 1.05019 | .00063 |
| .3000 | 1.74407 | .11455 | 1.82266 | .08791 | 1.55462 | 0.00000 | 1.05380 | .00152 |
| .3371 | 1.60283 | .08146 | 1.66557 | .05816 | 1.51506 | 0.00000 | 1.05259 | .00184 |
| .5500 | 1.00000 | .05693 | 1.00000 | .03652 | 1.00000 | 0.00000 | 1.00000 | .00506 |
| .6943 | .75250 | .04951 | .72525 | .02994 | .70633 | 0.00000 | .94949 | .00791 |
| 1.0600 | .42038 | .05610 | .35481 | .03278 | .28867 | 0.00000 | .61456 | .01829 |
| 1.5360 | .24176 | .04838 | .15449 | .02357 | .09994 | .00019 | .66051 | .03728 |
| 2.0000 | .14875 | .01909 | .05475 | .00210 | .04184 | .00127 | .54380 | .06158 |
| 2.2500 | .13430 | .01997 | .04044 | .00842 | .02728 | .00159 | .49133 | .07533 |
| 2.5000 | .12316 | .02042 | .03082 | .00867 | .01948 | .00291 | .44677 | .08943 |
| 2.7000 | .13237 | .05399 | .64620 | .03139 | .01335 | .00405 | .41671 | .10051 |
| 3.0000 | .12228 | .04050 | .05272 | .03949 | .06513 | .05880 | .38063 | .11614 |
| 3.3923 | .10700 | .01447 | .01867 | .00646 | .08930 | .08297 | .34778 | .13310 |
| 3.7500 | .10108 | .00867 | .01266 | .00316 | .06532 | .06019 | .32904 | .14348 |
| 4.5000 | .09308 | .01496 | .01127 | .00595 | .04766 | .04519 | .29722 | .14633 |
| 5.0000 | .08565 | .01336 | .00866 | .00519 | .04278 | .04133 | .27506 | .13728 |
| 5.5000 | .07950 | .01627 | .00886 | .00646 | .05810 | .05703 | .25082 | .12462 |
| 6.0000 | .07276 | .02342 | .01449 | .01304 | .05367 | .05266 | .22620 | .11184 |
| 6.2000 | .07377 | .02421 | .01399 | .01247 | .04392 | .04304 | .21652 | .10709 |
| 6.5000 | .07353 | .02435 | .01228 | .01095 | .03342 | .03285 | .20253 | .10076 |
| 7.0000 | .07854 | .03517 | .01728 | .01620 | .04456 | .04437 | .17266 | .09006 |
| 7.2000 | .04651 | .02828 | .01475 | .01449 | .11867 | .11816 | .14905 | .08734 |
| 8.0000 | .04451 | .03916 | .02285 | .02278 | .14709 | .14633 | .14234 | .09000 |
| 8.7000 | .12176 | .06739 | .03215 | .02930 | .12734 | .12639 | .14082 | .10304 |
| 9.0000 | .12693 | .07280 | .03494 | .03184 | .09291 | .09215 | .15057 | .11905 |
| 9.2000 | .12808 | .08086 | .04285 | .04053 | .08778 | .08722 | .16399 | .13437 |
| 10.0000 | .09102 | .04013 | .01452 | .01544 | .05019 | .04968 | .23605 | .19531 |
| 10.5910 | .08020 | .03206 | .01304 | .01234 | .04070 | .04044 | .24461 | .20095 |
| 11.0000 | .07424 | .02662 | .01101 | .01044 | .05734 | .05739 | .27791 | .22494 |
| 11.5000 | .06880 | .02530 | .01120 | .01076 | .03576 | .03551 | .25076 | .18418 |
| 12.5000 | .06155 | .02524 | .01297 | .01272 | .01975 | .01962 | .15272 | .09285 |
| 14.8000 | .05285 | .03046 | .01753 | .01741 | .01892 | .01892 | .09801 | .06665 |
| 15.0000 | .06173 | .04292 | .02468 | .02462 | .01956 | .01949 | .09456 | .06323 |

```

16.4000 .06260 .03469 .01741 .01722 .03665 .03665 .14576 .12329
17.2000 .07159 .03975 .01766 .01747 .04152 .04146 .12373 .10551
18.5000 .05959 .03260 .01513 .01506 .01715 .01709 .18348 .16184
21.3000 .06212 .03684 .01557 .01551 .01620 .01620 .12190 .09835
25.0000 .05325 .03387 .01456 .01456 .00835 .00835 .12924 .10592
30.0000 .04703 .03391 .01532 .01532 .00633 .00633 .08338 .06759
40.0000 .04393 .03455 .01582 .01582 .00589 .00589 .04108 .03247

***** CONTINUUMS ARE INTERIM (04/24/79) *****
0 * LBLF4 *
DV FOR LBLF4 = 1.58080 BOUND FOR LBLF4 = 25.2928
0 FIRST LINE USED IN RDLIN4 --- CHECK THE LINEFIL
EOF CN LINEFIL IN RDLIN4 --- CHECK THE LINEFIL
0
TIME
1.247
READ CONVOLUTION .007
PANEL 0.000
0 * HIRAC1 *
OUTPUT CN FILE 10 DV = .02470000 BOUNDF3(CM-1) = 6.3232
FIRST LINE ON LINEFIL USED (MORE LINES MAY BE REQUIRED)
* EOF CN LINEFIL (MORE LINES MAY BE REQUIRED)
1025 2095.000000 .21251308E+00
1026 2095.024700 .23875292E+00
1429 2104.978800 .71545200E-01
1430 2105.003500 .72624964E-01
0
TIME
1.608
READ CONVOLUTION .308
PANEL .004
0 AVERAGE WIDTH = .08651 AVERAGE ZETA = .97602 NO. LINES = 823 NO. CHANGES = 0
1 2095.000000 .50861183E-07 .80854974E+00
2 2095.024700 .56718727E-07 .78760946E+00
405 2104.978800 .16037268E-07 .93095420E+00
406 2105.003500 .16308452E-07 .92994953E+00
TIME REQUIRED FOR --EMINIT-- .013
1
0 DATA FOR FASCODE2 REPORT, GROUND TO 20 KM, VERTICAL, AEROSOLS ON FASCODE1 80/08/01. 14.43.04.
0 LAYER = 2
0 PRESS(MB) = 846.59847
0 TEMP(K) = 278.39
0 SECANT = 1.00000
H20 = 1.173E+22
CO2 = 7.225E+20
O3 = 6.777E+16
N2O = 6.130E+17
CO = 1.642E+17
CH4 = 3.503E+18
O2 = 4.586E+23
N2 = 1.709E+24
WKAER = .79164E-01
0 SELF BROADENING FACTOR FOR H2O IS 1.02153
0 COMPUTED DV BEFORE MODIFICATION = .02202022
TYPE OF PATH = 1
RATIO OF PREVIOUS DV TO CURRENT DV = 1.1217
TYPE OF MERGE 0
0 DV FOR THE LAYER .02470000
***** CONTINUUMS ARE INTERIM (04/24/79) *****
0 * LBLF4 *

```

DV FOR LBLF4 = 1.53080 BOUND FOR LBLF4 = 25.2923
 0 FIRST LINE USED IN RDLIN4 --- CHECK THE LINEFIL
 EOF ON LINEFIL IN RDLIN4 -- CHECK THE LINEFIL
 0
 TIME 1.672
 READ .007
 CONVOLUTION .006
 PANEL .001
 0 * HIRAC1 *
 OUTPUT ON FILE 10 DV = .02470000 BOUND3(CX-1) = 6.3232
 FIRST LINE ON LINEFIL USED (MORE LINES MAY BE REQUIRED)
 EOF ON LINEFIL (MORE LINES MAY BE REQUIRED)
 1025 2095.000000 .13796026E+00
 1026 2095.024700 .15373386E+00
 1429 2104.972800 .45239949E-01
 1430 2105.003500 .45928005E-01
 0
 TIME 1.986
 READ .000
 CONVOLUTION .272
 PANEL .003
 0 AVERAGE WIDTH = .07752 AVERAGE ZETA = .97360 NO. LINES = 823 NO. CHANGES = 0
 0 THE TIME AT THE START OF RADPRG IS 1.997
 1 2095.000000 .71114184E-07 .70435442E+00
 2 2095.024700 .78416337E-07 .67537528E+00
 405 2104.972800 .23376408E-07 .83977643E+00
 406 2105.003500 .23763079E-07 .83920477E+00
 0 THE TIME AT THE END OF RADPRG IS 2.002
 .015 SECS WERE REQUIRED FOR THIS MERGE

FINAL LAYER

1 DATA FOR FASCOD2 REPORT, GROUND TO 20 KM, VERTICAL-AEROSOLS ON
 0 FASCOD1 80/09/01. 14.43.04.
 0 LAYER = 20

0 PRESS(MB) = 59.98000
 0 TEMP(K) = 215.60
 0 SECANT = 1.00000

H20 = 1.471E+18
 CO2 = 6.607E+19
 O3 = 4.573E+17
 N2O = 5.606E+16
 CO = 1.501E+16
 CH4 = 3.203E+17
 O2 = 4.195E+22

N2 = 1.563E+23
 0 WKAER = .58479E-03
 0 SELF BROADENING FACTOR FOR H2O IS 1.00003
 0 COMPUTED DV BEFORE MODIFICATION = .00184575
 TYPE OF PATH = 1
 RATIO OF PREVIOUS DV TO CURRENT DV = 1.3549
 TYPE OF MERGE 3

0 DV FOR THE LAYER .00187566
 0 ***** CONTINUUMS ARE INTERIM (04/24/79) *****

0 * L3LF4 *
 DV FOR L3LF4 = .12004 READ CONVOLUTION .044
 TIME 9.406
 0 * HIRAC1 *
 OUTPUT ON FILE 10 DV = .00197566
 -1) = .4802

BOUND F3(CM

1025 2095.000000 .97030616E-01
 1026 2095.001876 .91536800E-01
 2431 2097.637173 .23440367E-02
 2432 2097.639048 .24933910E-02
 33 2097.640924 .26649310E-02
 34 2097.642800 .28632146E-02
 2431 2102.138748 .31801572E-02
 2432 2102.140623 .34120511E-02
 33 2102.142499 .37118442E-02
 34 2102.144375 .41323181E-02
 1555 2104.997248 .91982734E-02
 1556 2104.999123 .75425034E-02

0 TIME READ CONVOLUTION PANEL
 9.653 .002 .183
 0 AVERAGE WIDTH = .00682 AVERAGE ZETA = .77955 NO. LINES
 464 NO. CHANGES = 0

```

0 THE TIME AT THE START OF RAMPING IS 9.651
1 2095.000000 .5544851E-07 .55880728E+00
2 2095.061876 .56321764E-07 .56444128E+00
1497 2097.637173 .76539018E-07 .59110297E+00
1498 2097.639043 .75806442E-07 .59297272E+00
1 2097.640924 .75230149E-07 .59467820E+00
2 2097.642806 .74533068E-07 .59618765E+00
2399 2102.138748 .24917037E-07 .82871025E+00
2400 2102.140623 .24892769E-07 .82776311E+00
1 2102.142499 .24842629E-07 .82634380E+00
2 2102.144375 .24795136E-07 .82495850E+00
1523 2104.997248 .27755935E-07 .79083859E+00
1524 2104.999123 .27340110E-07 .79446629E+00
0 THE TIME AT THE END OF RAMPING IS 9.898
.244 SECS WERE REQUIRED FOR THIS RAMP
1. DATA FOR FASCD02 REPORT, GROUND TO 20 NM, VERTICAL AEROSOLS ON
FASCD01 90/08/01. 14.43.04.
0 SECANT = 0.00000
0 PRESS(ME) = 59.76000
0 TEMP(N) = 215.60
0 DV(CM-1) = .00187566
0 V1(CM-1) = 2095.000000
0 V2(CM-1) = 2105.000000
0 LAYER = 20
0 COLUMN DENSITY (MOLECULES/CM**2)
H2O = 4.737E+22
CO2 = 6.701E+21
O3 = 3.530E+18
N2O = 5.685E+18
CO = 1.523E+18
CH4 = 3.249E+19
O2 = 4.254E+24
0*** SINCSQ ***
INPUT FILE NUMBER = 12, JENIT = 0 JFN = 3
HUBM OF INSTRUMENT FUNCTION = 1.00000000 CM-1
ROUND OF INSTRUMENT FUNCTION = 4.52000000 CM-1
OUTPUT FILE NUMBER = 11, V1 = 2095.10000, V2 = 2104.95000
DV GUT .25000000
NF = 226, DXF = .02000, SUM = .997456312531470
SHRINK RATIO = 16
END OF FILE ENCOUNTERED
0 TIME = 9.969, READ = .004, CONV. = .052, PANEL = 0.000
0 SUMIN = .641322358E+01
1
0 V1P = 2095.10000 V2P = 2104.85000 DVOUT = .25000000 NLIM =
40
0
.36382E+00 .44527E+00 .51555E+00 .56811E+00 .59998E+00 .61144E+
00 .60729E+00 .59449E+00 .58093E+00 .57293E+00
0
.68123E+00 .67045E+00 .66034E+00 .65082E+00 .63952E+00 .62191E+
00 .59325E+00 .54967E+00 .49009E+00 .41674E+00
SUMOUT .589029948E+01
EOI.
E>

```

APPENDIX B: FASCOD2-82 PROGRAM REVISIONS AND USERS GUIDE

The code designated FASCOD2-82 is based on the AFGL code FASCOD1B of May, 1981. Modifications have been made in order to (1) adjust the far wing CO₂ lineshape using a new fourth subfunction form factor CHI and a new continuum and (2) allow non-LTE line strengths to be used at high altitude in both transmittance and radiance calculations.

In the case of CO₂, the fourth function lineshape is now computed separately from the other gases. The same program lineshape control parameters apply. These govern which of the Lorentz subfunctions are used, and the various combinations are enumerated below:

IHIRAC=1 allows the line-by-line summation algorithm to be used with the three subfunctions F1, F2, and F3 which cover the region within 64 halfwidths of line center (for all molecules).

ILBLF4=1 adds the fourth subfunction F4 (if IHIRAC=1) to the first three subfunctions. F4 is modified by the exponential form factor CHI in the case of CO₂ only.

ICNTNM=1 adds the scaled "fifth" or remainder continuum subfunction for CO₂, N₂, and water vapor.

The following summary shows the structure of program routines related to the fourth and "fifth" subfunctions. The asterisk indicates where FASCOD2-82 routines contain significant changes. These program changes for the sub-Lorentzian CO₂ lineshape have been largely confined to the routines SHRINK, CONV4, and the CO₂ continuum data subroutine FRNCO2.

LBLF4 ROUTINES

LBLF4 Fourth function driver. Scales line strengths by column density amounts and temperature correction factors. Calculates P and T adjusted halfwidths ALFAD and ALFAV. Modifies R4 by radiation field term and returns R4 to LAYER for later merger with ABSRB, R3, R2, and R1.

VOICON Computes the Voigt profile factor AVRAT(IZETA) .

MOLEC Computes line strength (SCOR) and Lorentz halfwidth (ALFCOR) correction factors from P and T. Also calculates the Doppler halfwidth (ALFD1) at GNU=1.

RDLIN4 Up to 1250 lines are loaded into the arrays GNU(I), S(I), ALFAL(I), ALFAD(I) and MOL(I).
* The Non-LTE vibrational transition index is stripped from the MOL array.
BUFIN is called to read blocked line data from TAPE3.

SHRINK Merges nearby lines together to form fewer effective lines.
* CO₂ and non-CO₂ lines are 'lumped' separately.
Returns the new line data:
 GNU(J) strength-weighted average frequency
 S(J) summed line strength for merged lines
 ALFAL(J) strength-weighted Lorentz halfwidth
 ALFAD(J) strength-weighted Doppler halfwidth
 * MOL(J) molecular ID =0 for non-CO₂ lines
 =2 for CO₂ lines

CONVF4 Performs line-by-line fourth function sum to produce the R4 array.
* Uses a Lorentz subfunction F4 which is modified by the exponential form factor CHI for CO₂ lines only.

RADFN Returns the value of the radiation field term.

CONTINUUM ROUTINES

| | |
|--------|--|
| CONTNM | Scales/interpolates stored continuum data and loads the array ABSRB. |
| SLF296 | Stored self-broadened H_2O continuum for T=296 K. |
| SLF260 | Stored self-broadened H_2O continuum for T=260 K. |
| FRN296 | Stored foreign-broadened H_2O continuum for T=296 K. |
| FRNCO2 | * Stored foreign-broadened CO_2 continuum for T=296 K. Includes the sub-Lorentz 'REMAINDER' subfunction. |

CONT Called by HIRAC to merge ABSRB and R4 into R3.

The non-LTE calculation uses a straightforward extension of the HIRAC line-by-line algorithm, which is made to perform two line-by-line convolutions simultaneously. An entirely new program branch (bearing the interim name HIRACQ) is activated at high altitudes to perform the non-LTE calculations if the user specifies INLTE=1. The new branch routines HIRACQ, CNVFNQ, and PANELQ are the non-LTE analogs of HIRAC1, CNVFNV, and PANEL. The new subroutine STRTHS is used by HIRACQ to compute the two "effective strengths" for each line which is enhanced or diminished by the non-thermal vibrational populations. The vibrational populations of H_2O , CO_2 , O_2 , and NO are functions of altitude and are read directly from the appropriate output file of the Degges and Smith high altitude computer model. The populations read from this file are used to calculate the vibrational state population enhancement ratios by the subroutine RDPOPS. The ratios are stored for use by STRTHS. The actual single-layer radiance calculation is performed by EMIN, which has been modified to calculate radiance from the two HIRACQ line-by-line absorption and "effective absorption" spectral

functions. A summary of these routines with brief descriptions are given below:

NON-LTE ROUTINES

| | |
|---------|--|
| BCDNLTE | Prepares a blocked line file for use in the non-LTE calculation. Vibrational state labels are coded and added to the molecular ID for each non-equilibrium line. |
| RDPOPS | Reads the file containing non-LTE population data. Calculates population enhancement ratios. |
| HIRACQ | Performs two separate line-by-line calculations. |
| STRTHS | Computes the effective line strength for absorption and for the second function C. Returns these two strengths to HIRACQ for each line. |
| CONVFNQ | Constructs the arrays (R1,R2,R3; RR1,RR2,RR3) which are needed for the two line-by-line sums. |
| PANELQ | Merges the two separate sets of subfunctions and writes the spectral functions K and C to a temporary file. |
| EMIN | Calculates the single layer radiance and transmittance from the spectral functions K and C. |

The off-line program BCDNLTE prepares the blocked line data file for use by FASCOD2 in doing non-LTE calculations. In addition to formatting the line data (frequency, strength, halfwidth, lower state energy, and molecular ID), this program sorts the lines into equilibrium and non-equilibrium transitions, and then adds two vibrational state code numbers to the molecular ID. The code numbers are presently based on the order of states used in the model of Degges and Smith, but can be altered to allow use with other non-LTE gas models in the future. More details about program BCDNLTE can be found in Appendix C.

On the next two pages a sample job submission file is presented. This file can be used to compile and execute FASCOD2-82 if the molecular data has been prepared previously by BCDNLTE. Output from BCDNLTE has been stored in file "NLTELINEFILE" in this example. File "BASEVIBPOP", the Degges and Smith output file, contains the needed vibrational population data.

The listing below illustrates two job features. The SEGLOAD tree can be used to segment the program for execution with about 70K of space on the AFGL CDC 6600 computer. The tree shows the hierarchy of program subroutines and the disposition of various COMMON blocks. The last eight lines also present a sample job INPUT card sequence. The program control parameters and data which appear will not be described in detail here since only one change has been made to the corresponding card sequence for version FASCOD1B. The single additional parameter (INLTE) appears at the end of card 2 (EQ=0). In this case the non-equilibrium option has been turned off, so that HIRACQ will not be executed since the run is to be made for a (equilibrium) sea level horizontal path.

<TOP OF FILE>

SCRAF,CM70000,T45.

USER

REQUEST/P1/*PF.

ATTACH(TAPE3,NLTELINFILE,ID=USER,MR=1)

ATTACH(TAPE7,BASEVIBPOP,ID=USER,MR=1)

ATTACH(PROG,FASCOD2,ID=USER,MR=1)

FTN(I=PROG,B=PROGB,L=L,T,ER)

EXIT(U)

MAP,PART.

LDSET,PRESET=INDEF.

LOAD,PROGB.

SEGLOAD.

EXECUTE,FASCOD1.

EXIT(U)

REWIND,OUTPUT.

COPYCF,OUTPUT,P1.

CATALOG(P1,FASCOD2OUT,ID=USER)

EOR

FASCODE TREE FASCOD1-(LAYRS,LASER,SCANFN,PLOTT,FLTRFN,TEST)

FASCOD1 GLOBAL CONSTS,FILHDR,MAIN

FASCOD1 INCLUDE FASCOD1,BUFIN,BUFOUT

*

LAYRS TREE LAYER-(PATH,HIRAC1,HIRACQ,LBLEF4,CONTNW,ABSMRG,EMINIT,
,RADMRG,AERSOL)

LAYER GLOBAL ABSORB,SCATTR,LBLEF4,LINHDR,VBNLTE-SAVE

LAYER INCLUDE LAYER,RADFN,RDPOPS,SKIP

*

PATH INCLUDE PATH

PATH GLOBAL PATH-SAVE

*

HIRAC1 INCLUDE HIRAC1,SHAPEL,SHAPEQ,VOICON,RDLIN,CNVFNV,PANEL,MOLEC,
,QV,CONT,ABSOUT,VERFN,R1PRNT,XINT

HIRACQ INCLUDE HIRACQ,SHAPEL,SHAPEQ,VOICON,RDLIN,CNVFNQ,PANELQ,
,MOLEC,QV,CONT,ABSOUT,VERFN,R1PRNT,XINT,STRTHS

HIRAC1 GLOBAL FNS-SAVE

HIRACQ GLOBAL FNSQ-SAVE,XRNLTE-SAVE

*

LBLEF4 INCLUDE LBLEF4,RDLIN4,CONVF4,MOLEC,QV,SHRINK,VOICON

*

CONTNW TREE CONTNM-(SLF296,SLF260,FRN296,FRNCO2,N2CONT)

CONTNM INCLUDE CONTNM,XINT

SLF296 INCLUDE SLF296

SLF260 INCLUDE SLF260

FRN296 INCLUDE FRN296

FRNCO2 INCLUDE FRNCO2

N2CONT INCLUDE N2CONT

*

ABSMRG INCLUDE ABSMRG,ABSOUT

```

*
EMINIT  INCLUDE  EMINIT,EMIN,EMOUT,BBFN
*
RADMRG  INCLUDE  RADMRG,EMIN,EMOUT,BBFN
*
SCANFN  INCLUDE  SCANFN,SHAPEG,RDSCAN,SHRKSC,SHAPET,CONVSC,PANLSC,
,CNVREC,SINCSQ,CKPRNT
*
FLTRFN  INCLUDE  FLTRFN,RDSCAN,CNVFLT
*
TEST    INCLUDE  TEST
*
PLOTT   TREE     PLTFAS-(HEADER,AXEST,FPLINE)
PLTFAS  GLOBAL   PLTHDR,AXISXY,YCOM,POINTS,CHEXP,TITLOC,NAME
PLTFAS  INCLUDE  PLTFAS,LINT,EXPT,XNTLOG,TEMPFN,TENLOG,MNMX,LINT
*
AXEST   TREE     AXES-(AXISL,AXLOG,AX2)
        END      FASCOD1
EOR
1      5.1 KM SEA LEVEL HORZNTL
      HI=1 F4=1 CN=1 AE=0 EM=1 SC=0 FI=0 PL=0 TS=0 EQ=0
      2350.000 2400.000
      0.000
      0.000
      1
      1013.0000 288.1000
      1.006E+23 4.254E+21 3.456E+17 3.610E+18 9.670E+17 2.063E+19 2.701E+24 1.007E+25
      <BOTTOM OF FILE>

```

APPENDIX C : PROGRAM BCDNLTE

Program BCDNLTE prepares molecular line data in blocked BCD computer card images for use with the non-LTE subroutines of FASCOD2-82. The program has been constructed using program BCDMRG as a basis, and making only a few modifications so as to permit identification of non-LTE transitions by FASCOD2. The user should note that program BCDMRG is completely compatible with FASCOD2 under circumstances where only equilibrium conditions (low altitude) are to be specified. Furthermore, if the input parameter INLTE is set equal to zero, BCDNLTE will function identically with BCDMRG.

Both BCDNLTE and BCDMRG create line data files for a specified spectral range for use by FASCOD2. This data includes each line's frequency, intensity and half-width at 296°K, lower state energy level, and a molecular ID between 1 and 20 which is used to distinguish the various gases. BCDNLTE must also pass to FASCOD2 information to allow the identification of the upper or lower vibrational states, if either or both of those states is non-thermally populated at high altitude. This additional information is passed through the last variable MOL, which in BCDMRG is the molecular identifier. In the non-LTE mode, MOL has the 6-digit integer from IJKLMN, where MN is the ordinary molecular ID, IJ and KL are upper and lower vibrational state identifiers, respectively. Either IJ or KL will be zero if the upper or lower vibrational state doesn't match one of the non-equilibrium vibrational states, or if MN is not the ID of a

non-equilibrium gas. The user should note, however, that modifications will also be required to FASCOD2 subroutine RDPOPS in order to use a revised set of vibrational states in non-LTE calculations. Appendix B provides a description of this routine.

The identification of the upper and lower vibrational state of each line, and comparison with the non-equilibrium states of the model of Degges and Smith is accomplished in subroutine VIBQU. This routine is called once for each line. Standard vibrational state ID's are compared against the specific non-equilibrium state ID's which have been stored in array DATA statements. If a match occurs, the corresponding number (presently from 1-10) is added to the proper digits of MOL (forming MOL2 from MOL1 in VIBQU). The number of non-equilibrium vibrational states is currently taken to be 8 for water vapor, 10 for carbon dioxide, 2 for ozone, and 3 for nitric oxide. In each case, the ground state is included first. Updating and modification of the selected set of vibrational states for each gas can be done simply by modifying the two DATA statements within VIBQU which initialize NUMH2O, NUMCO2, NUMO3, NUMNO, and HVQH2O, HVQCO2, HVQO3, HVQNO.

C.1 SAMPLE FILE FOR THE SUBMISSION OF BCDNLTE

```

<TOP OF FILE>
SCRAF,T300,MT2.
REQUEST/BCDOUT/TAPE3/*PF.
ATTACH(PROG,BCDNLTE,ID=USER)
FTN,I=PROG,B=PROGB,T,ER.
VSN(TAPE1=CC0157)
LABEL(TAPE1,R,L=CC0157)
VSN(TAPE2=CC0171)
LABEL(TAPE2,R,L=CC0171)
COPYCF,TAPE1,DUM,22.
COPYCF,TAPE2,DUM,22.
PROGB.
EXIT(U)
CATALOG(TAPE3,NLTELINEFILE,ID=USER)
EXIT(U)
REWIND,OUTPUT.
COPYCF,OUTPUT,BCDOUT.
CATALOG(BCDOUT,BCDNLTEOUT,ID=USER)
RETURN(TAPE1)
RETURN(TAPE2)
EXIT(U)
EOR
RUN OF BCDNLTE FOR USE IN NLTE CALCULATIONS
2300.000 2450.000 INLTE= 1
11111111111111111111 TAPE1
11111111111111111111 TRACE
<BOTTOM OF FILE>

```

C.2 PROGRAM BCDNLTE: LISTING OF SUBROUTINE VIBQU

SUBROUTINE VIBQU(LTEMP)

C
C
C
C
C
C
C
C
C
C

THIS SUBROUTINE COMPARES THE TWO VIBRATIONAL LEVEL
ID'S OF SELECTED MOLECULES AGAINST STORED VIB STATE
ID'S. MOL IS ADJUSTED TO INCLUDE ADDITIONAL IDENTIFIERS.

IJ ----- UPPER STATE ID
KL ----- LOWER STATE ID
MN ----- ORDINARY MOLECULAR ID

COMMON TI7(7),TI10(10),RO,R(320)
DIMENSION HVQH20(8),HVQC02(10),HVQ03(2),HVQNO(3)
EQUIVALENCE (TI7(7),MOL2)
EQUIVALENCE (TI10(5),VIB1),(TI10(6),VIB2),(TI10(10),MOL1)
DATA NUMH20,NUMC02,NUM03,NUMNO/8,10,2,3 /
DATA (HVQH20(I),I=1,8)/

1 6H 0 0 0,
2 6H 0 1 0,
3 6H 0 2 0,
4 6H 1 0 0,
5 6H 0 0 1,
6 6H 0 3 0,
7 6H 1 1 0,
8 6H 0 1 1 /

DATA (HVQC02(I),I=1,10)/

1 10H 0 0 0 0 1,
2 10H 0 1 1 0 1,
3 10H 1 0 0 0 2,
4 10H 0 2 2 0 1,
5 10H 1 1 1 0 2,
6 10H 0 3 3 0 1,
7 10H 1 0 0 0 1,
8 10H 0 0 0 1 1,
9 10H 1 0 0 1 2,
C 10H 1 0 0 1 1 /

DATA (HVQ03(I),I=1,2)/

1 6H 0 0 0,
2 6H 0 0 1 /

DATA (HVQNO(I),I=1,3)/1H0,1H1,1H2 /

C
C
C
C
C
C

MOL1 IS THE ORIGINAL MOLECULAR ID
MOL2 IS THE NEW TAGGED MOL ID

MOL2=MOL1

IF(MOL1.NE.1) GO TO 200

```

C
C  WATER VAPOR LINE
C
      REWIND LTEMP
      WRITE(LTEMP,900) (TI10(J),J=5,9)
C
      REWIND LTEMP
      READ(LTEMP,901) VIB1,VIB2
900  FORMAT(5A7)
901  FORMAT(21X,A6,1X,A6)
      NUPP=0
      DO 150 NVQ=1,NUMH2O
      HTEST=HVQH2O(NVQ)
      IF (VIB1.NE.HTEST) GO TO 150
      NUPP=NVQ
      GO TO 160
150  CONTINUE
160  NLOW=0
      DO 170 NVQ=1,NUMH2O
      HTEST=HVQH2O(NVQ)
      IF (VIB2.NE.HTEST) GO TO 170
      NLOW=NVQ
      GO TO 180
170  CONTINUE
180  MOL2 = MOL1 + 100*NLOW + 10000*NUPP
      GO TO 500
200  CONTINUE
      IF(MOL1.NE.2) GO TO 300
C
C  CO2 LINE
C
      REWIND LTEMP
      WRITE(LTEMP,900) (TI10(J),J=5,9)
      REWIND LTEMP
      READ(LTEMP,902) VIB1,VIB2
902  FORMAT(2X,A10,5X,A10)
      NUPP=0
      DO 250 NVQ=1,NUMCO2
      HTEST=HVQCO2(NVQ)
      IF (VIB1.NE.HTEST) GO TO 250
      NUPP=NVQ
      GO TO 260
250  CONTINUE
260  NLOW=0
      DO 270 NVQ=1,NUMCO2
      HTEST=HVQCO2(NVQ)
      IF (VIB2.NE.HTEST) GO TO 270
      NLOW=NVQ
      GO TO 280
270  CONTINUE

```

```

280  MOL2 = MOL1 + 100*NLOW + 10000*NUPP
      GO TO 500
300  CONTINUE
C
      IF(MOL1.NE.3) GO TO 400
C
C  OZONE LINE
C
      REWIND LTEMP
      WRITE(LTEMP,900) (TI10(J),J=5,9)
      REWIND LTEMP
      READ(LTEMP,903) VIB1,VIB2
903  FORMAT(21X,A6,1X,A6)
      NUPP=0
      DO 350 NVQ=1,NUMO3
      HTEST=HVQO3(NVQ)
      IF (VIB1.NE.HTEST) GO TO 350
      NUPP=NVQ
      GO TO 360
350  CONTINUE
360  NLOW=0
      DO 370 NVQ=1,NUMO3
      HTEST=HVQO3(NVQ)
      IF (VIB2.NE.HTEST) GO TO 370
      NLOW=NVQ
      GO TO 380
370  CONTINUE
380  MOL2 = MOL1 + 100*NLOW + 10000*NUPP
      GO TO 500
C
400  CONTINUE
      IF(MOL1.NE.8) GO TO 500
C
C  NITRIC OXIDE LINE
C
      REWIND LTEMP
      WRITE(LTEMP,900) (TI10(J),J=5,9)
      REWIND LTEMP
      READ(LTEMP,904) VIB1,VIB2
904  FORMAT(7X,A1,7X,A1)
      NUPP=0
      DO 450 NVQ=1,NUMNO
      HTEST=HVQNO(NVQ)
      IF (VIB1.NE.HTEST) GO TO 450
      NUPP=NVQ
      GO TO 460
450  CONTINUE
460  NLOW=0
      DO 470 NVQ=1,NUMNO
      HTEST=HVQNO(NVQ)

```

```

      IF (VIB2.NE.HTEST) GO TO 470
      NLOW=NVQ
      GO TO 480
470   CONTINUE
480   MOL2 = MOL1 + 100*NLOW + 10000*NUPP
500   CONTINUE
C
      DO 550 J=1,6
      TI7(J)=TI10(J)
550   CONTINUE
      RETURN
      END

```